



# Recent Progress of Metal-Organic Framework-Based Photodynamic Therapy for Cancer Treatment

Yuyun Ye, Yifan Zhao, Yong Sun , Jie Cao 

Department of Pharmaceutics, School of Pharmacy, Qingdao University, Qingdao, 266021, People's Republic of China

Correspondence: Jie Cao; Yong Sun, Email [caojie0829@qdu.edu.cn](mailto:caojie0829@qdu.edu.cn); [sunyong@qdu.edu.cn](mailto:sunyong@qdu.edu.cn)

**Abstract:** Photodynamic therapy (PDT), combining photosensitizers (PSs) and excitation light at a specific wavelength to produce toxic reactive oxygen species, has been a novel and promising approach to cancer treatment with non-invasiveness, spatial specificity, and minimal systemic toxicity, compared with conventional cancer treatment. Recently, numerous basic research and clinical research have demonstrated the potential of PDT in the treatment of a variety of malignant tumors, such as esophageal cancer, bladder cancer, and so on. Metal-organic framework (MOF) has been developed as a new type of nanomaterial with the advantages of high porosity, large specific surface area, adjustable pore size, and easy functionalization, which could serve as carriers to load PSs or increase the accumulation of PSs in target cells during PDT. Moreover, active MOFs have the potential to construct multifunctional systems, which are conducive to refining the tumor microenvironment (TME) and implementing combination therapy to improve PDT efficacy. Hence, a comprehensive and in-depth depiction of the whole scene of the recent development of MOFs-based PDT in cancer treatment is desirable. This review summarized the recent research strategies of MOFs-based PDT in antitumor therapy from the perspective of MOFs functions, including active MOFs, inactive MOFs, and their further combination therapies in clinical antitumor treatment. In addition, the bottlenecks and obstacles in the application of MOFs in PDT are also described.

**Keywords:** photodynamic therapy, metal-organic framework, tumor microenvironment, active MOFs, inactive MOFs

## Introduction

About 100 years ago, Tappeiner studied that the phenomenon of PS combined with light killing cells was oxygen-dependent, and proposed the concept of photodynamic effect for the first time to describe this oxygen-dependent photosensitization reaction.<sup>1,2</sup> The emergence of this concept has attracted extensive attention from scientists and researchers, which has greatly promoted the development of PDT.<sup>3</sup> Nowadays, PDT has been widely used in the treatment of many diseases<sup>4–8</sup> including malignant tumors<sup>9,10</sup> for its non-invasiveness, spatial specificity, and minimal side effect on normal tissues. Typically, under the irradiation of a certain wavelength of light, PS absorbs a certain amount of light energy to become an excited PS. Subsequently, the absorbed energy transfers to the adjacent oxygen ( $O_2$ ), and the  $O_2$  are excited into highly toxic reactive oxygen species (ROS), including superoxide anion radical ( $O_2^{\cdot-}$ ), hydroxyl radical ( $\cdot OH$ ), hydrogen peroxide ( $H_2O_2$ ), and singlet oxygen ( $^1O_2$ ).<sup>11</sup> ROS,<sup>12</sup> especially cytotoxic  $\cdot OH$  and  $^1O_2$ , can be effective antitumor species by penetrating the cell membrane and then reacting with biological macromolecules (such as proteins and nucleic acids) in the tumor cell to induce cell apoptosis or necrosis.<sup>11,13</sup> Thus, worldwide researchers have focused on developing PSs for effective PDT.

Commonly used PSs in clinical PDT are from three families<sup>14</sup> — porphyrins,<sup>15</sup> chlorophylls,<sup>16</sup> and organic dyes.<sup>17</sup> However, most PSs are hydrophobic, lack targeting, and have low bioavailability, so using PS in vivo is prone to self-aggregation, fluorescence quenching, and phagocyte scavenging by the mononuclear phagocyte system, which usually fails to achieve the desired antitumor effect of PDT. In recent years, with the development of nanotechnology,<sup>18</sup> nanocarriers,<sup>19</sup> such as liposomes,<sup>20–22</sup> dendrimer,<sup>23–25</sup> nanomicelles,<sup>26–28</sup> nanohydrogel,<sup>29–31</sup> have been greatly used for improving the safety and

effectiveness of PSs, due to their advantages of effective targeting, delayed-release, improved cargo stability, reduced systemic toxicity and avoidance of premature clearance. However, most nanocarriers have disadvantages such as poor drug loading, poor biocompatibility, nonrepeatability, and poor stability. For example, although liposomes with good biocompatibility have a unique bilayer structure, which can simultaneously upload hydrophilic drugs and hydrophobic drugs, they could not achieve locally controlled release, and have poor stability.<sup>32</sup> Dendrimers have the advantages of monodispersity, easy functionalization, and biodegradation, but their wide application is limited by high cost and single type, so current studies are mostly based on PAMAM and polyethyleneimine (PEI) dendrimers.<sup>33</sup>

Nanoscale metal-organic frameworks (NMOFs) are a new porous nanocarrier with an organic-inorganic hybrid, which has been attracted more and more attention in biomedical fields.<sup>34</sup> By comparison to traditional nanocarriers, MOFs have many unique properties in drug loading and delivery. Firstly, some MOFs have a response-degradation mechanism, which is conducive to the effective release of drugs in tumors.<sup>35–37</sup> For example, ZIF-8, a kind of pH-responsive MOF from the zeolitic imidazolate frameworks (ZIF) family, could collapse in tumor cells due to its low pH and release its cargos. Secondly, compared with the other drug carriers, such as liposomes, micelles, dendrimers, and inorganic carriers, MOFs showed high drug loading properties and low systemic toxicity.<sup>35,38–42</sup> Thirdly, MOFs also show great potential in disease diagnosis.<sup>43</sup> MOFs and their hybrids as nanosensors have high selectivity, stability, reproducibility, and reusability, which is beneficial to the early diagnosis of tumors.<sup>44–46</sup>

In the past decade, the research of MOFs in the field of PDT had been soaring promptly. UiO NMOF<sup>47</sup> which is from the University of Oslo (UiO) family was introduced into PDT in 2014, ZIF NMOF<sup>48</sup> in 2015, and PCN NMOF<sup>49,50</sup> from the porous coordination network (PCN) family in 2019. When PS acts as a ligand of MOFs, MOFs show increased near-infrared absorption compared to PSs alone, due to isolation of PSs and enhanced intersystem crossings (ISCs), resulting in increased ROS production. They can be used as a new class of highly effective PSs with intrinsic photodynamic therapy. When used as drug delivery nanocarriers,<sup>51</sup> which is to say, loading or connecting PSs directly, MOFs present more of their advantages, such as high drug loading, prevention of premature leakage, high bioavailability, etc., to implement efficient non-intrinsic photodynamic therapy. Hence, MOFs can be divided into two categories, active MOFs and inactive MOFs, depending on whether they have other functions besides being carriers. Inactive MOFs are mostly used as carrier materials for PDT, while active MOFs can play other roles in assisting treatment and achieve more ideal therapeutic effects while performing carrier functions. As shown in Table 1, compared with PDT produced by free PSs, MOFs-based PDT has a better antitumor therapeutic effect in vivo. In addition, MOFs can also serve as excellent nanoplatforms for conducting combination therapies, such as chemotherapy (CT), radiotherapy (RT), and starvation therapy.

Various reviews have summarized MOFs-based PDT in preclinical applications, mainly focusing on the construction or modification of MOFs,<sup>58–60</sup> but few reviews are focusing on MOFs-based photodynamic therapy in terms of the function of MOF itself. Therefore, a comprehensive and in-depth depiction of the whole scene of the recent

**Table 1** In vivo Antitumor Effect of Free Photosensitizer and MOFs-Based PDT

Free Photosensitizer	TGI (Tumor Growth Inhibition) Value	MOFs-Based PDT	TGI Value	Ref
5,15-di (p-benzoato) porphyrin (H <sub>2</sub> DBP)	–25%	DBP-UiO	98%	[47]
5,15-di (p-benzoato) chlorin (H <sub>2</sub> DBC)	17% in CT26 models; 14% in HT29 models	DBC-UiO	88% in CT26 models; 68% in HT29 models	[52]
5,10,15,20-tetra (p-benzoate) porphyrin (H <sub>4</sub> TBP)	33%	Ti-TBP	98%	[53]
5,10,15,20-tetra (p-benzoate) bacteriochlorin (H <sub>4</sub> TBB)	43% in 4T1 models; 57% in MC38 models	Zr-TBB	94% in 4T1 models; 99% in MC38 models	[54]
H <sub>2</sub> BDC	9%	TMPyP4-G4-aptamer-NMOFs	95%	[55]
Ce6	49%	Ce6@ZIF-8	94%	[56]
Ce6	50%	MCOPP-NE-Ce6	90%	[57]

development<sup>60</sup> of MOFs-based PDT in cancer treatment is desirable. This review has summarized the recent research strategies of MOFs-based PDT in antitumor therapy from the perspective of MOFs functions, including active MOFs, inactive MOFs, and their further combination therapies in clinical antitumor treatment (Figure 1). Moreover, the review has more focused on the application of active MOFs in PDT antitumor therapy, especially the research work on intrinsic photodynamic MOFs. In addition, the obstacles to the application of MOFs in clinical PDT are also discussed.

## MOFs

### Concept of MOFs

MOFs are materials with porous networks of one-dimensional, two-dimensional, or three-dimensional structures formed by coordination between inorganic metal ions or clusters and nitrogen-containing or carboxylic acid multidentate organic ligands, also known as porous coordination polymers.

### Characteristics of MOFs

MOFs with high porosity, high surface area, adjustable pore size, easy functionalization, good biocompatibility, and biodegradability, are a kind of promising drug delivery carriers. Due to their unique characteristics, MOFs exhibit great potential in drug delivery.

### The Advantages of MOFs as Drug Carriers

#### High Drug Loading

MOFs exhibited high drug loading due to high surface area and good physicochemical stability.<sup>38</sup> A large number of drug molecules could enter into channels and firmly loaded on the MOFs through coordination with metal ions or hydrophobic interaction with organic ligands. As a drug delivery carrier, MOFs can be developed for single drug delivery<sup>61</sup> or even dual-drug delivery.<sup>62</sup> Moreover, MOFs can deliver the vast majority of drugs without any requirements on the physicochemical properties of the drugs.<sup>40</sup> As a result, MOFs can load with small drug molecules, peptides,<sup>63,64</sup> and even biological macromolecules.<sup>65</sup> MOFs with high drug loading could improve the biological toxicity, in vivo metabolism, and stability problems that may be caused by a large number of carriers.

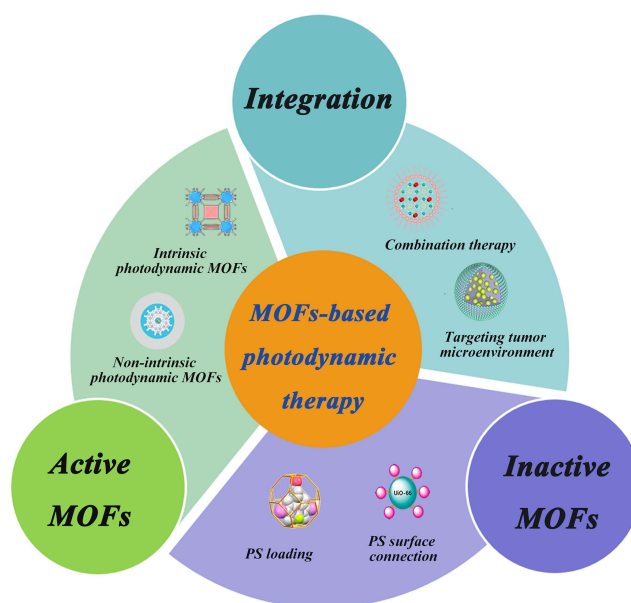


**Figure 1** The framework of MOFs-based photodynamic therapy.

## Stimuli-Responsive Degradation

Among all stimuli-responsive MOFs, pH-responsive MOFs are the most commonly studied, because of their sensitivity to the tumor microenvironment. ZIF-8 is the most common pH-sensitive MOF. Zhuang et al<sup>66</sup> reported on a platelet cell membrane-coated ZIF-8 for the targeted delivery of siRNA *in vivo*. ZIF-8 was capable of high loading, and its pH-responsive characteristic endowed endosomal disruption, releasing siRNA. There are other stimuli-responsive MOFs, such as magnetically-responsive MOFs, ion-responsive MOFs, temperature-responsive MOFs, and pressure-responsive MOFs.<sup>34</sup> In addition to single-stimuli-responsive MOFs, multi-stimuli-responsive MOFs have emerged due to the complexity of the tumor. Ni et al<sup>67</sup> encapsulated doxorubicin (DOX) into double-layer NH<sub>2</sub>-MIL-88B from the Materials of Institute Lavoisier (MIL) family to realize the pH and glutathione (GSH) dual-responsive controlled DOX release.

## Synthesis Methods of MOFs

MOF is mainly a combination of metal ions and organic ligands. Metal parts, also known as metal nodes, are usually composed of metals and oxygen atoms, hydroxyl groups, carboxylic acids, etc. The organic ligand component is mostly polycarboxylic acids.

The classical synthesis method of MOF is solvo (hydro)-thermal method<sup>68</sup> which needs to be carried out under severe high temperature and pressure conditions. Therefore, in recent years, some new synthesis methods have been developed successively, such as the microwave-assisted method, mechanochemical method, and electrochemical method.<sup>69</sup> Besides solvo (hydro)-thermal method, the microwave-assisted method is the preferred method to synthesize MOFs in the lab, compared with the conventional hydrothermal method, because microwave synthesis greatly shortens the synthesis time and improves the efficiency. The mechanochemical method is to prepare MOFs by forming new coordination with mechanical forces. Its main advantages are green, efficient and economical. Electrochemical method is the preferred method for the industrial synthesis of MOFs. External voltage is applied to make organic ligand ions move towards the anode and coordinate with metal ions in the reaction solution. The advantage of electrochemical method is that the reaction temperature is lower than that of solvo-thermal method. The reaction conditions are mild and the reaction speed is fast (Figure 2).

## Active MOFs

Active MOFs are a class of MOFs with functionality, including intrinsic photodynamic MOFs, Fenton MOFs, REDOX MOFs, and other active MOFs.

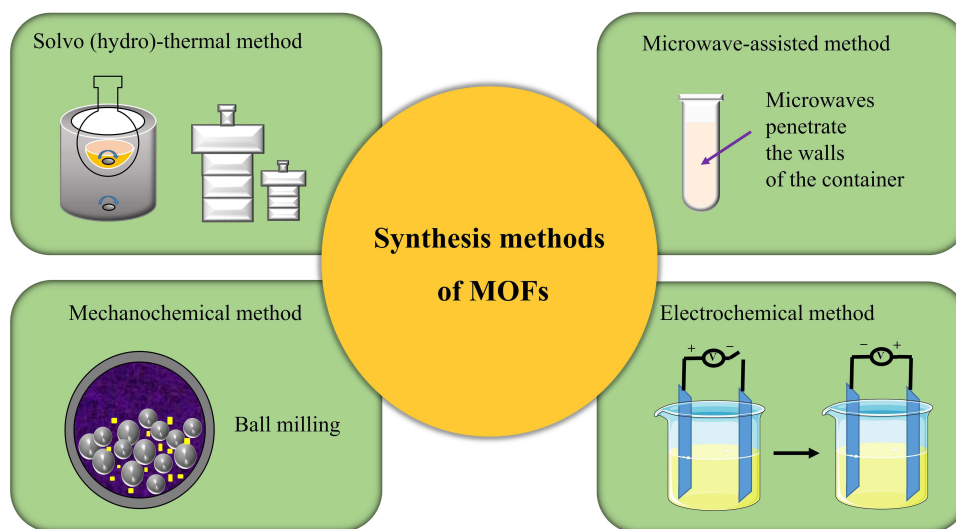


**Figure 2** The illustration of synthesis methods of MOFs.



## Intrinsic Photodynamic MOFs

Intrinsic photodynamic MOFs contain PSs as their ligand and metal nodes. PSs are arranged regularly and orderly in the MOFs to improve photostability, which makes better use of O<sub>2</sub> and produces more <sup>1</sup>O<sub>2</sub>. Intrinsic photodynamic MOFs are expected to realize more ROS production than PSs themselves, achieving better PDT efficacy.

### Porphyrin-Based MOFs

Porphyrins and their derivatives have been widely used in PDT as PSs, and directly using porphyrins and their derivatives as organic ligands is a common method to prepare intrinsic photodynamic MOFs. The porphyrin molecules arrange in the skeleton of MOFs are highly regular, which improves the hydrophobicity, further prevents the self-aggregation of porphyrin molecules, and increases the generation of <sup>1</sup>O<sub>2</sub>. Not only can the structure of MOFs enhance the drug loading of porphyrin molecules,<sup>70</sup> but also facilitate the entry of O<sub>2</sub> and the diffusion of <sup>1</sup>O<sub>2</sub> to avoid self-quenching.<sup>71,72</sup> So far many researchers have synthesized porphyrin-based MOFs. They synthesized intrinsic photodynamic MOFs with porphyrins for use in PDT and its combination therapy.

In 2014, Lin et al<sup>47</sup> developed porphyrin-based MOFs, DBP-UiO which was the first successful use of porphyrin-based NMOF as the PS of PDT. DBP-UiO was prepared by solvo-thermal method, and composed of 5,15-di (p-benzoato) porphyrin (H<sub>2</sub>DBP) ligands and hafnium (Hf) as the metal center in which the loading of H<sub>2</sub>DBP could be up to 77 wt %. Besides, the absorption peaks of DBP-UiO were red-shifted, and ROS generation was at least two times higher over H<sub>2</sub>DBP. Due to site isolation of porphyrin ligands, enhanced ISC of Hf centers, and the convenient <sup>1</sup>O<sub>2</sub> diffusion in porous DBP-UiO nanoplates, DBP-UiO effectively generated <sup>1</sup>O<sub>2</sub> and displayed enhanced PDT efficacy and antitumor effects both in vitro and in vivo compared to H<sub>2</sub>DBP alone. This work represented NMOFs as a new class of highly effective PSs in the clinical treatment of cancers. Then in 2015, the same group designed the first chlorine-based nanomaterial DBC-UiO<sup>52</sup> by replacing H<sub>2</sub>DBP with H<sub>2</sub>DBC (Figure 3). DBC-UiO owned extremely high PS loading, crystallinity, framework stability, porosity, nanoplate morphology, and enhanced ISCs. Compared with DBP-UiO, the photophysical properties of chlorine-based DBC-UiO were improved, with a 13 nm red shift and an 11-fold increase in the extinction coefficient in the lowest-energy Q band, so that the efficiency of the <sup>1</sup>O<sub>2</sub> generation of DBC-UiO is three times that of DBP-UiO in two colon cancer cell lines resulting in more efficient PDT. Meanwhile, DBC-UiO also showed a stronger anticancer effect than DBP-UiO in two colorectal adenocarcinoma mouse models. This work also further elucidated that apoptosis and immunogenic cell death (ICD) contributed to PDT-induced cell killing based on DBC-UiO.

Besides Hf can be used as the metal center of the intrinsic photodynamic MOF, zirconium (Zr),<sup>73,74</sup> and manganese (Mn)<sup>75</sup> can also be used for the construction of the internal photodynamic MOF. In particular, Zr is the most commonly used in porphyrin-based MOF. Zhou et al<sup>76</sup> synthesized a series of Zr<sub>6</sub>-based porphyrinic MOF, PCN-228, PCN-229, and PCN-300 with high surface area mesoporous by using topological structural-guided strategies. This type of MOF used extended porphyrin linkers as ligands, which effectively prevented network interpenetration that MOF is prone to. In addition, the high connectivity of Zr<sub>6</sub> clusters gave MOF enhanced stability. The pore size of the synthesized MOF was in the range of 2.5 to 3.8 nm, and in particular, PCN-229 had the highest porosity. The work provided a new strategy for the construction of stable mesoporous porphyrin MOF. They also investigated the effect of the size of PCN-224 nanoparticles on size-dependent cell uptake and subsequent PDT, showing that the function of Zr-based porphyrinic MOF can be controlled by adjusting the size of MOF.<sup>77</sup> Meanwhile, it was also verified that the MOF formulation of the photosensitizer showed a better PDT effect than its small molecules. In addition, Zr<sub>6</sub> in Zr-MOF could coordinate with the carboxyl group of folate (FA), a commonly used ligand for targeting folate receptor abundant tumor cells, such as ovarian tumors, to realize an active targeting. Hence, the active targeting of MOF nanomaterials could be realized through the functionalized modification of MOF by FA, thus showing an enhanced PDT effect.

The post-synthetic surface modification of porphyrin-based MOFs can be an effective method to enhance PDT efficiency. At present, this strategy has also been widely used in PDT antitumor therapy of porphyrin MOFs,<sup>78</sup> such as cell-penetrating peptide modification,<sup>79</sup> folic acid (FA) modification,<sup>80,81</sup> hyaluronic acid (HA)<sup>82</sup> modification, erythrocyte membrane modification,<sup>83</sup> cancer cell membrane modification,<sup>75,84</sup> exosome modification,<sup>85</sup> metal nanoparticles modification,<sup>86</sup> nanoenzyme modification,<sup>87</sup> etc. Different surface modifications have different functions to porphyrin-based MOFs. For example, Zhang et al<sup>88</sup> modified catalase-like platinum nanoparticles (Pt NPs) on the surface of PCN-224

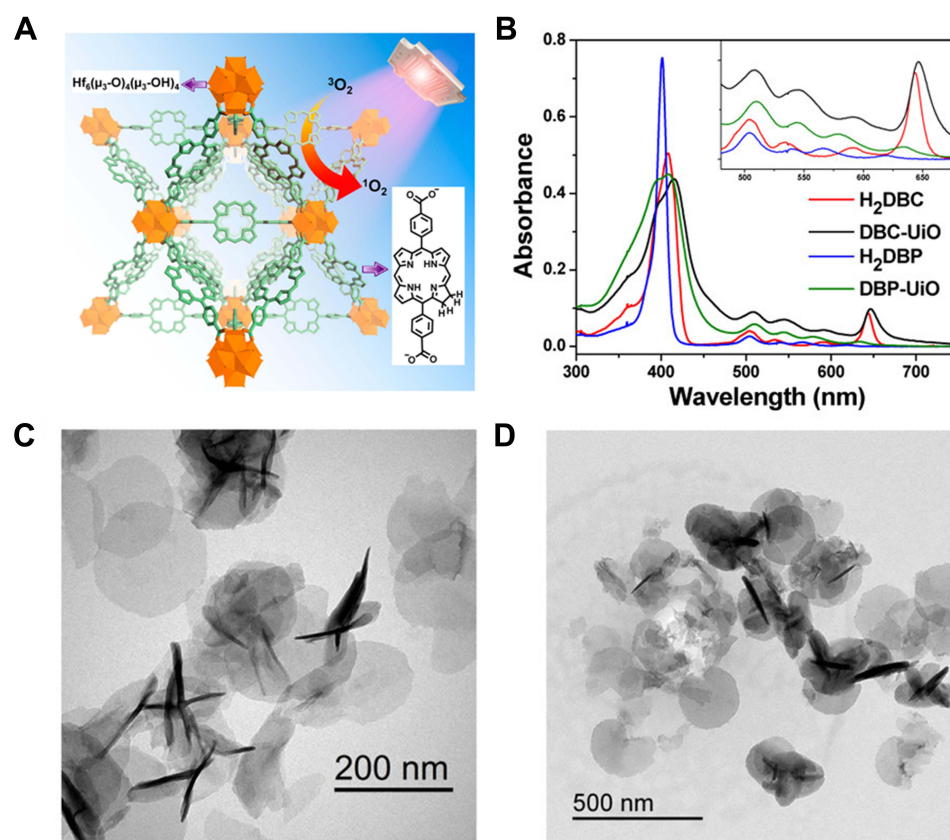


**Figure 3** Characterization and in vivo therapy results of DBC-UiO. (A) The Illustration of DBC-UiO of <sup>1</sup>O<sub>2</sub> Generation Process; (B) UV-vis absorption spectra of H<sub>2</sub>DBC, DBC-UiO, H<sub>2</sub>DBP, and DBP-UiO; (C and D) TEM images of DBC-UiO showing nanoplate morphology (C) before and (D) after incubation in cell culture medium. Reprinted with permission from Lu K, He C, Lin W. A Chlorin-Based Nanoscale Metal-Organic Framework for Photodynamic Therapy of Colon Cancers. *J Am Chem Soc.* 2015;137(24):7600–7603 Copyright (2015) American Chemical Society.<sup>52</sup>

for better capable of killing tumor cells. That catalyzed generation of <sup>1</sup>O<sub>2</sub> from excess H<sub>2</sub>O<sub>2</sub> in TME, promoted the formation of <sup>1</sup>O<sub>2</sub> in anoxic sites, and alleviated anoxic conditions. Min et al<sup>84</sup> used tumor cell membrane to camouflage and modify porphyrinic Zr-MOF, endowing it with biomimetic function and enabling it to homologous target tumor cells. After intravenous administration in mice, camouflaged nanoparticles selectively accumulated in tumors through homologous targeting ability mediated by biomimetic modifications.

Due to the extension of their  $\pi$ -conjugation, benzoporphyrin derivatives exhibit red-shifted absorption bands (at  $\lambda=700$  nm), so they have stronger infrared luminescence properties and higher chemical stability than conventional porphyrins.<sup>89</sup> Zeng et al<sup>90</sup> reported on a new  $\pi$ -extended benzoporphyrin-based MOF (TBP-MOF) (Figure 4A), with 10-connected Zr<sub>6</sub> cluster and much improved photophysical properties due to the  $\pi$ -extended benzoporphyrin-based linkers, which was better than traditional porphyrin-based MOFs. They applied 5,10,15,20-tetra (p-benzoate) porphyrin (H<sub>4</sub>TBP) for ligands. The tetrabenzoporphyrin-based linkers of TBP-MOF were well dispersed in the framework that avoids the self-quenching of the excited state. Compared with traditional porphyrin-based MOFs, TBP-MOF had higher chemical stability, red-shifted absorption bands, and stronger infrared luminescence characteristics. Further modification of TBP-MOF by poly (ethylene glycol) could better and more efficiently be applied in TME. It did not only induce apoptosis and necrosis of 4T1 murine breast cancer cells but also enhance the performance of tumor-antigens activated to T cells. At the same time, it was found that TBP-MOF mediated and low oxygen-dependent PDT combined with PD-L1 checkpoint blocking therapy could significantly inhibit the growth of the primary tumor, stimulate the systemic immune response, and inhibit the growth of metastatic tumor (Figure 4B).

Many scholars believe that the exploration of NMOFs in PDT should not be limited to an oxygen-dependent type II mechanism, because the hypoxic situation in TME will limit oxygen-dependent type II PDT, and the development

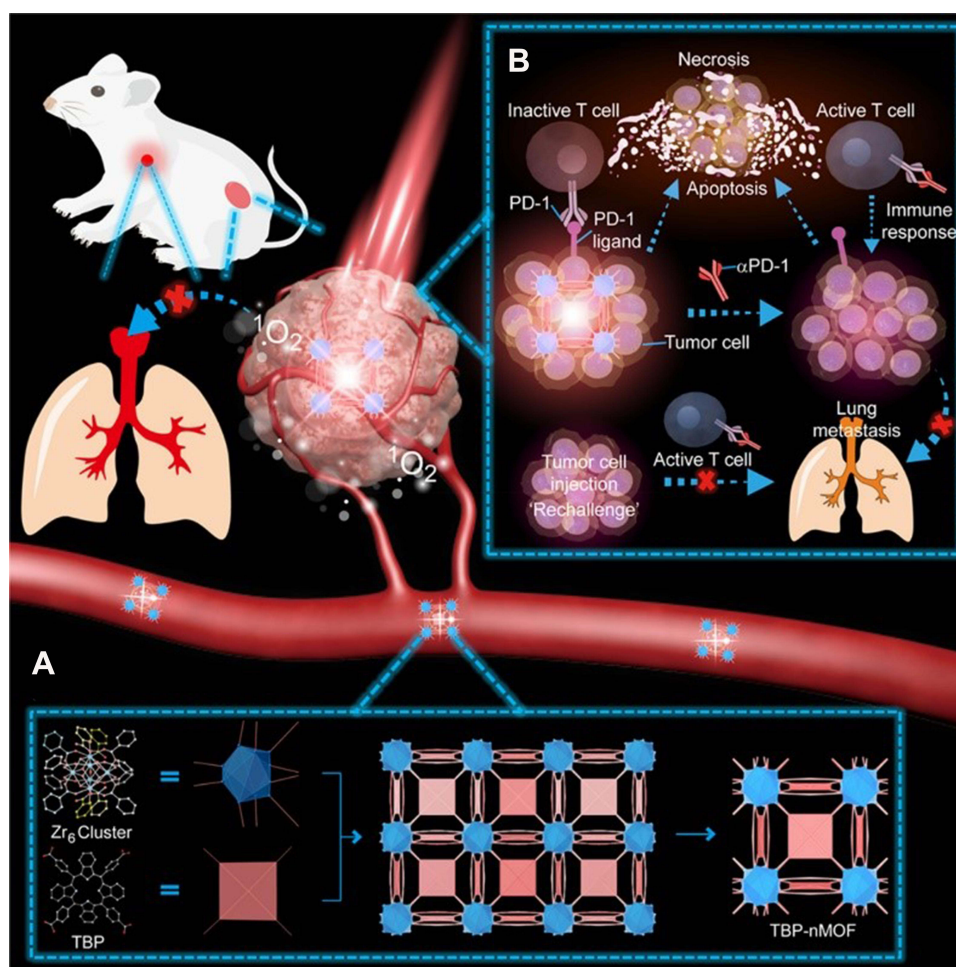


**Figure 4** The scheme of TBP-NMOF for inhibition of tumor metastasis. **(A)** The preparation process of TBP-NMOF; **(B)** TBP-NMOF-mediated photodynamic cancer immunotherapy. TBP-NMOF-mediated PDT induces an adaptive antitumor immune response that recruits tumor-infiltrating T cells to inhibit tumor metastasis. Reprinted with permission from Zeng JY, Zou MZ, Zhang M, et al.  $\pi$ -Extended Benzoporphyrin-Based Metal–Organic Framework for Inhibition of Tumor Metastasis. *ACS Nano*. 2018;12(5):4630–4640. Copyright (2018) American Chemical Society.<sup>90</sup>

of anoxic-tolerant type I PDT is a new promising strategy.<sup>91–93</sup> Based on benzoporphyrinic MOFs, Lin's group<sup>53</sup> worked on this and synthesized a new type of MOF, Ti-TBP, which consisted of Ti-oxo chain secondary building units (SBUs) and photosensitizing TBP ligands for hypoxia-tolerant type I PDT and oxygen-dependent type II PDT, and it applied for superb anticancer efficacy (Figure 5). Upon light irradiation, Ti-oxo chain SBUs were fairly close to TBP ligands in Ti-TBP (Figure 5A), which facilitated the electron transfer to generate  $\text{TBP}^{+}$  ligands and  $\text{Ti}^{3+}$  centers, increasing singlet oxygen production, including superoxide,  $^1\text{O}_2$ ,  $\text{H}_2\text{O}_2$  and  $\cdot\text{OH}$  (Figure 5B and C). Due to generating four distinct ROS, Ti-TBP-mediated PDT gave superb anticancer efficacy with > 98% tumor regression and 60% cure rate.

At present, intrinsic photodynamic MOFs are mainly based on porphyrins and their derivatives ligands. As we know, the introduction of heavy atoms (Br or I) into a PS has an impact on the ISC rates, the quantity of the  $^1\text{O}_2$  generation, and then the effect of PDT.<sup>94</sup> So, it is a great idea to make the incorporation of heavy atoms such as iodine (I) into PSs and even into MOFs, and it could meet the demands of the increased antitumor effect of PDT. Zhou et al<sup>95</sup> employed a one-pot synthetic approach to incorporate an iodine-attached Zn(II)-porphyrinic dicarboxylic building block ( $\text{ZnDTPP-I}_2\text{-2H}$ ) into UiO-66 NMOF to produce the  $\text{ZnDTPP-I}_2\text{@UiO-66}$  which could be a highly effective PS for treatment of liver cancer cells in vitro. This work proved that the conventional porphyrin with heavy iodine atoms could be successfully nanosized by employing NMOF supports. Meanwhile, it also provided a highly efficient PDT platform for treating liver cancer in which  $\text{ZnDTPP-I}_2\text{@UiO-66}$  was utilized as an effective PS.



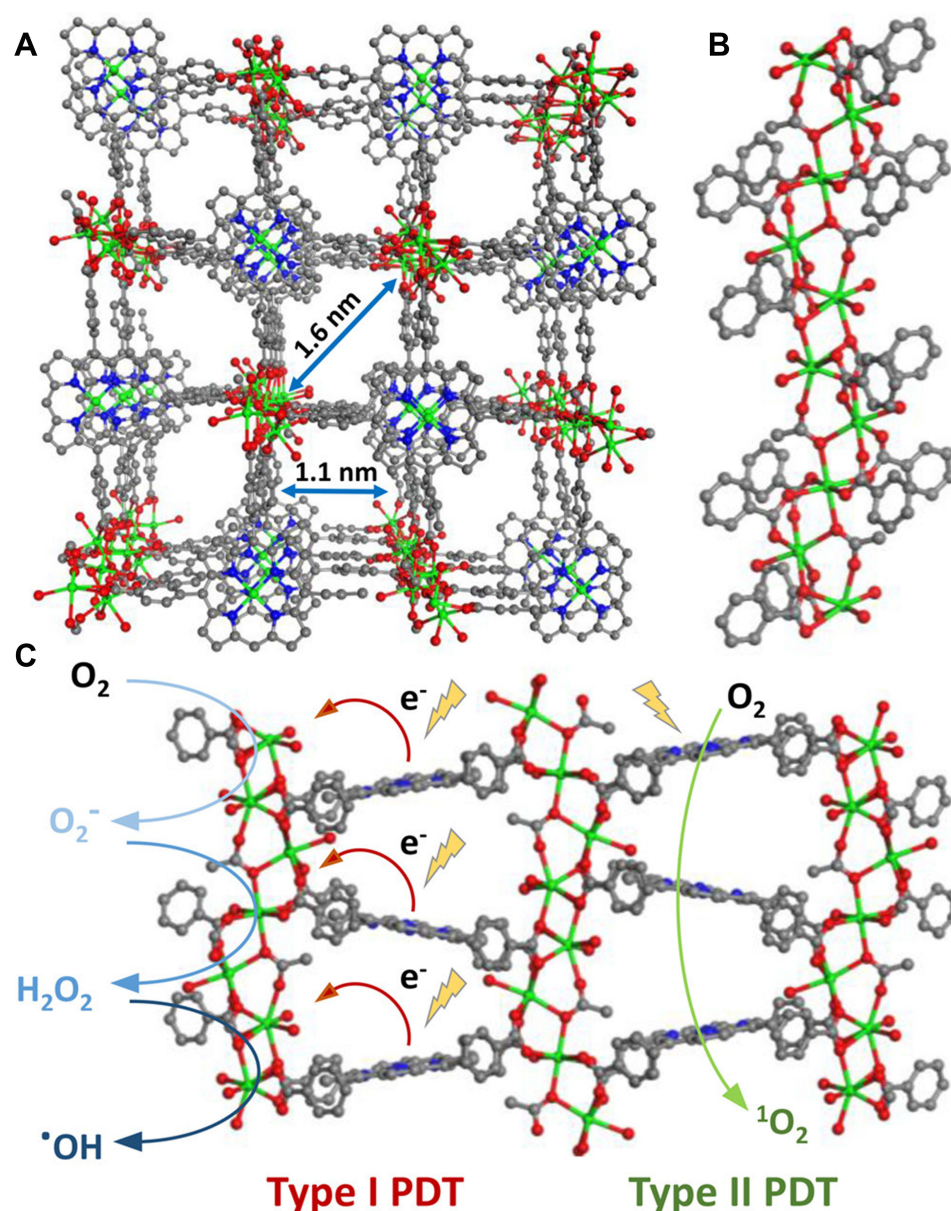


**Figure 5** (A) Perspective view of Ti-(Ti-TBP) structure along the (010) direction; (B) coordination environments of Ti-oxo chain SBUs; (C) Schematic showing both type I and type II PDT enabled by Ti-TBP. Reprinted with permission from Lan G, Ni K, Veroneau SS et al. Titanium-Based Nanoscale Metal-Organic Framework for Type I Photodynamic Therapy. *J Am Chem Soc.* 2019;141(10):4204–4208. Copyright (2019) American Chemical Society.<sup>53</sup>

### Bacteriochlorin-Based MOFs

Bacteriochlorin-based MOFs can also implement synchronous type I and type II PDT.<sup>96</sup> Lin's group<sup>54</sup> confirmed this idea in their research. They directly used both bacteriochlorin based on type II PDT as a PS and NMOF as a carrier to stabilize bacteriochlorin, realizing the synchronous type I and type II PDT (Figure 6A). NMOF (Zr-TBB) with PCN-224 structure was synthesized by solvo-thermal reaction that was composed of 5,10,15,20-tetra(p-benzoate) bacteriochlorin ( $H_4TBB$ ) and  $Zr^{4+}$ . Upon a 740nm laser, Zr-TBB showed excellent photostability, indicating that the stability of bacteriochlorin was improved significantly (Figure 6B–D). In vitro experiments showed that Zr-TBB could simultaneously perform type I and type II PDT, and accordingly produce superoxide anions ( $O_2^{\cdot-}$ ),  $H_2O_2$ ,  $\cdot OH$ , and  $^1O_2$ . Even in hypoxic conditions, Zr-TBB was still highly effective in killing cells. Zr-TBB showed good effects in the mouse model of breast cancer and colon cancer with 40% and 60% cure rates, respectively.

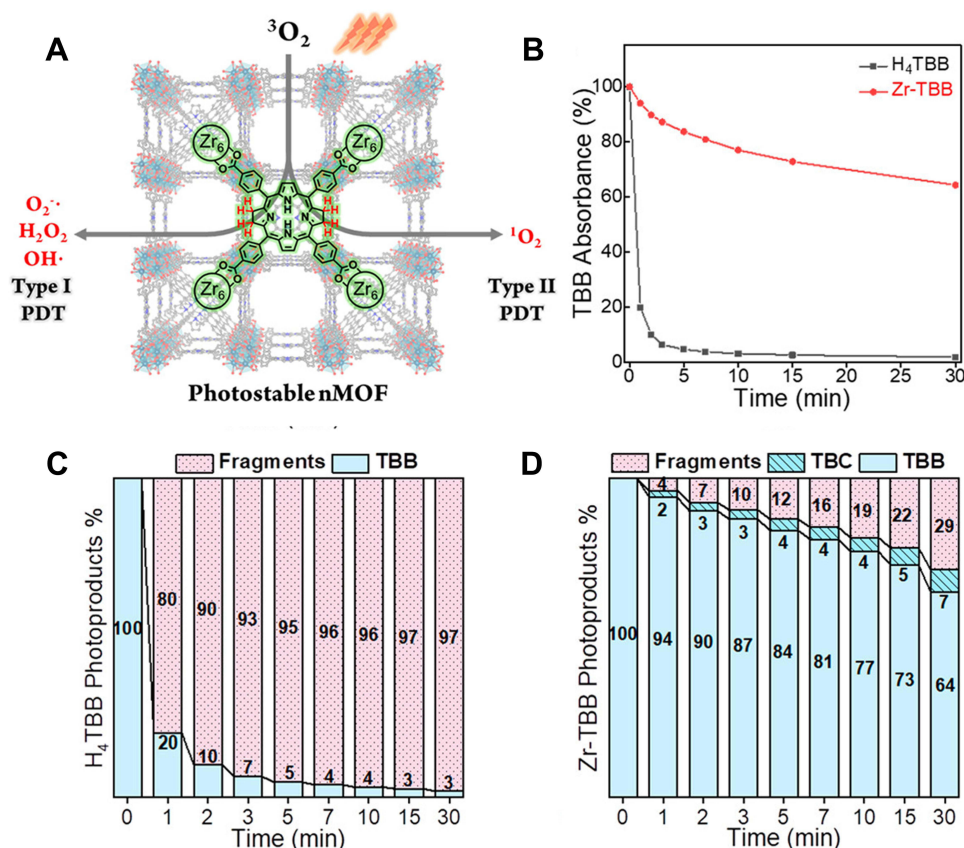


**Figure 6** (A) The illustration of bacteriochlorin ligands in Zr-TBB for Type I and Type II PDT to produce four species of reactive oxygen species; (B) time-dependent UV-visible absorption of TBB after light exposure in air-saturated DMF; the percentage of photoproducts (TBB, TBC, fragment) of H<sub>4</sub>TBB (C) and Zr-TBB (D) after 30 minutes of light irradiation. Reprinted with permission from Luo T, Ni K, Culbert A et al. Nanoscale Metal-Organic Frameworks Stabilize Bacteriochlorins for Type I and Type II Photodynamic Therapy. *J Am Chem Soc.* 2020;142(16):7334–7339. Copyright (2020) American Chemical Society.<sup>54</sup>

## BODIPY-Based MOFs

BODIPY is a kind of new PSs that is different from porphyrin, chlorins, and bacteriochlorin. It has ideal PS characteristics, such as high extinction coefficient, photobleaching resistance, the low dark toxicity.<sup>97</sup> Compared with BODIPY, halogenated BODIPY enhances ISC and increased the <sup>1</sup>O<sub>2</sub> generation due to the heavy atom effect. Wang et al<sup>98</sup> first halogenated the carboxyl group of BODIPY to synthesize diiodide-substituted BODIPY (I<sub>2</sub>-BDP) and then incorporated I<sub>2</sub>-BDP into UiO-66 through solvent-assisted ligand exchange (SALE) to synthesize MOF (UiO-PDT) with PDT effect. The crystal structure, morphology, and size of UiO-PDT remained unchanged when I<sub>2</sub>-BDP replaced the original phenyldicarboxylate (H<sub>2</sub>BDC) of UiO-66 by efficient SALE, and UiO-PDT demonstrated low dark toxicity, high cell uptake, good biocompatibility, and high <sup>1</sup>O<sub>2</sub> production.

## Monodispersed Copper (I)-Based MOFs

It has been verified that in the presence of H<sub>2</sub>O<sub>2</sub>, CuTz-1 shows semiconductor properties and high photocatalytic activity. And it also produces ·OH efficiently by Fenton-like reaction.<sup>99</sup> In addition, CUTZ-1 also exhibits continuous absorption from visible light to the near-infrared (NIR) region, so CuTz-1 can be excited by 808 nm. Cai et al<sup>100</sup> prepared CuTz-1 by solvo-thermal method and coated it with amphiphilic polymer F127 to prepare CuTz-1@F127 (Figure 7A). CuTz-1@F127 itself was used as PS. In the presence of H<sub>2</sub>O<sub>2</sub>, it produced ·OH that belonged to type I PDT. In addition, CuTz-1@F127 carried O<sub>2</sub> molecules (CuTz-1-O<sub>2</sub>@F127) into tumor cells and adsorbed intracellular GSH through the coordination of unsaturated Cu (I) and strong coordination between Cu (I) and sulfhydryl group, respectively. CuTz-1@F127 alleviated both hypoxia and high GSH while it played a role in PDT. ROS and hypoxia production in cells were detected by fluorescence probe (Figure 7B), which confirmed that CuTz-1-O<sub>2</sub>@F127 could alleviate hypoxia and promote ROS production.

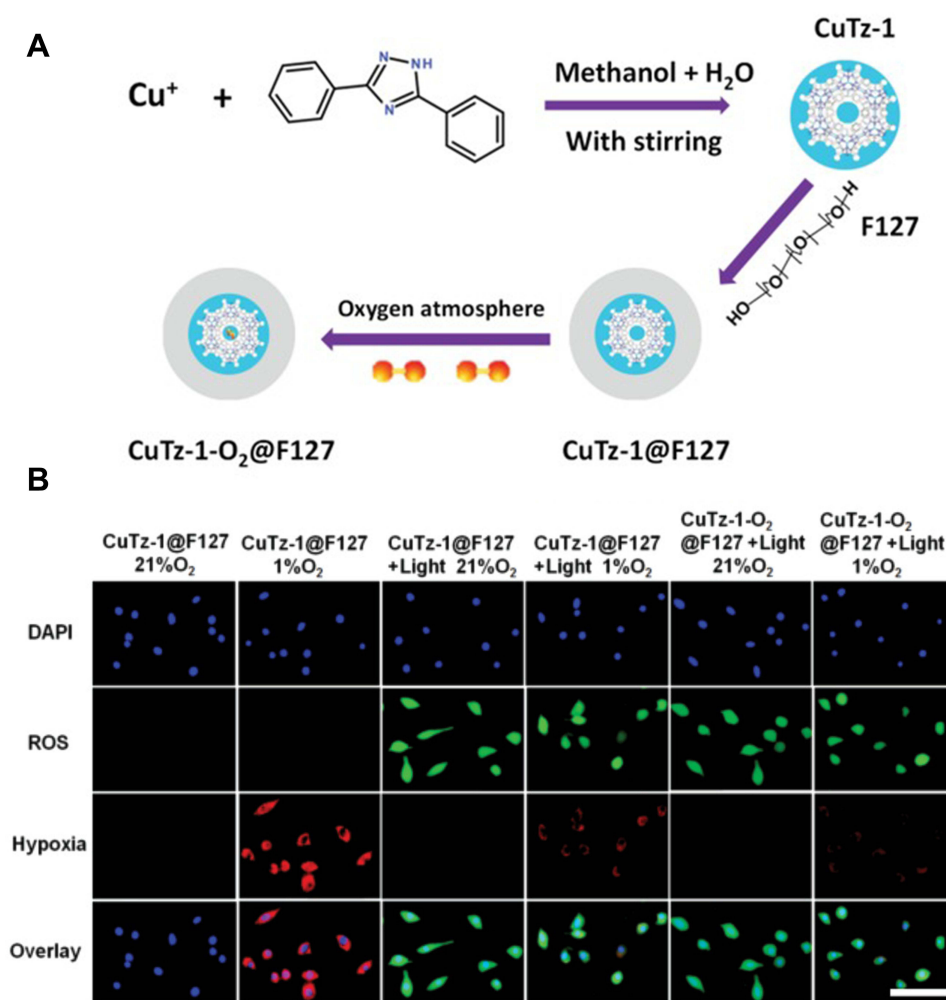


**Figure 7** (A) The illustration of preparation process of CuTz-1-O<sub>2</sub>@F127 and (B) ROS and hypoxia generation in cells after incubation with CuTz-1@F127 or CuTz-1-O<sub>2</sub>@F127 with or without 808 nm laser irradiation. Scale bar is 50  $\mu$ m. Reprinted from Cai X, Xie Z, Ding B et al. Monodispersed Copper(I)-Based Nano Metal-Organic Framework as a Biodegradable Drug Carrier with Enhanced Photodynamic Therapy Efficacy. *Advanced science* (Weinheim, Baden-Wurttemberg, Germany). 2019;6(15):1,900,848. © 2019 The Authors. Published by WILEY-VCH Verlag GmbH & Co. KGaA, Weinheim. Creative Commons license and disclaimer available from: <http://creativecommons.org/licenses/by/4.0/legalcode>.<sup>100</sup>

## Non-Intrinsic Photodynamic MOFs

### Fenton MOFs

Iron-based MOFs are one of the commonly used active MOFs. Since the introduction of iron ions can effectively catalyze H<sub>2</sub>O<sub>2</sub> in TME, the Fenton reaction that generates  $\cdot$ OH or O<sub>2</sub> occurs. Pei et al<sup>101</sup> constructed an iron-based porphyrin MOF (FeTCPP/Fe<sub>2</sub>O<sub>3</sub>) loaded with Fe<sub>2</sub>O<sub>3</sub> (Figure 8). The introduction of iron metal nodes effectively catalyzed the Fenton reaction to generate  $\cdot$ OH, and the supported Fe<sub>2</sub>O<sub>3</sub> overcame the hypoxic environment by generating O<sub>2</sub>. Synergistic treatment of  $\cdot$ OH and <sup>1</sup>O<sub>2</sub> generated by PDT improved tumor treatment effect. In addition, the Fenton reaction of iron-based MOF further alleviated hypoxia of TME.<sup>102</sup> Luo et al<sup>103</sup> used the porosity and multifunctionality of iron-based MOFs to build nanoplateforms. Not only can MIL-100 (Fe) support zinc phthalocyanine (ZnPc) and DOX, but also undergo Fenton-like reactions to produce O<sub>2</sub> by catalyzing H<sub>2</sub>O<sub>2</sub>. Upon 660 nm light irradiation, ZnPc effectively produced ROS due to the reduction of hypoxia by MIL-100 (Fe).

### REDOX MOFs

Redox metal ions such as Mn (IV) and Cu (II) are prone to oxidize GSH and reduce intracellular GSH levels, which promotes PDT in tumor cells. Similarly, MOFs containing these metal ions will also benefit from GSH consumption



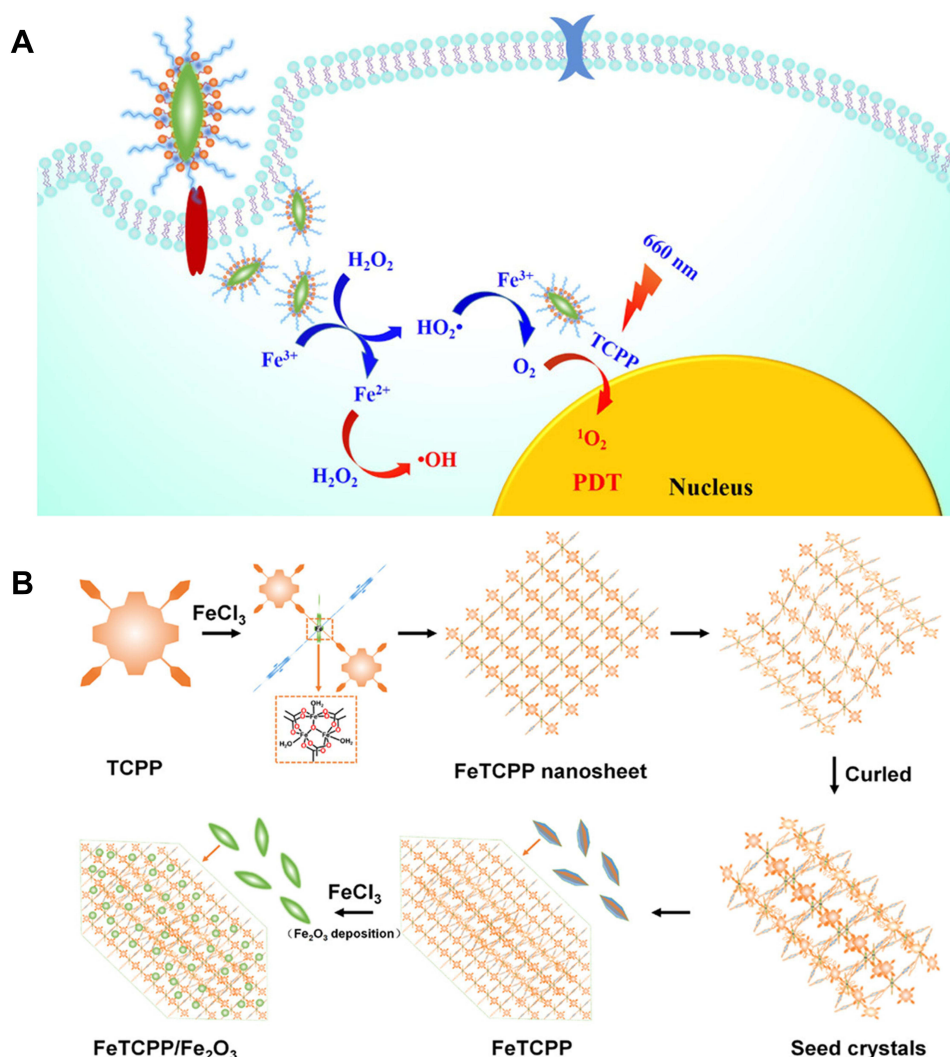


**Figure 8 (A)** The mechanism of FeTCPP/Fe<sub>2</sub>O<sub>3</sub> exerting antitumor efficacy for enhanced PDT; **(B)** formation mechanism of the FeTCPP and FeTCPP/Fe<sub>2</sub>O<sub>3</sub> MOF Nanorice. Reprinted with permission from Zhao Y, Wang J, Cai X, Ding P, Lv H, Pei R. Metal-Organic Frameworks with Enhanced Photodynamic Therapy: Synthesis, Erythrocyte Membrane Camouflage, and Aptamer-Targeted Aggregation. *ACS Appl Mater Interfaces*. 2020;12(21):23,697–23,706. Copyright (2020) American Chemical Society.<sup>101</sup>

and improve PDT performance. Considering Cu (II)-based MOF can effectively remove endogenous GSH,<sup>104</sup> Tang's group<sup>105</sup> constructed MOF-2 based on Cu (II) as the active center and the porphyrin ligand as the PS, which specifically bound and absorbed GSH by Cu (II) to directly decrease the intracellular GSH concentration and produced high levels of ROS for PDT under light conditions. Decreasing intracellular GSH synergistically produced higher ROS concentration and accelerated cell apoptosis, thus enhancing the antitumor efficiency of PDT. For its ability to adsorb GSH, MOF-2 alone (without light) can produce antitumor efficacy similar to that of camptothecin (CPT), a commercial antitumor drug. This work effectively demonstrated that MOF-2 could be used as a PDT candidate as well as an antitumor agent. Liu et al<sup>106</sup> used a Cu (II) carboxylate-based MOF-199 loaded with PSs to synthesize PS@MOF-199 (Figure 9A). Cu (II) as the metal center of MOF-199 could be used as a PS activation switch and GSH scavenger to activate PS and consume GSH to ensure that the ROS produced by PS was fully used for PDT (Figure 9B).

REDOX MOFs can also directly generate O<sub>2</sub> by catalyzing H<sub>2</sub>O<sub>2</sub>, which avoids the addition of subsequent O<sub>2</sub> supplement materials and is conducive to the improvement of stability.<sup>107</sup> Tang's group<sup>108</sup> designed and prepared a new PS with high photosensitivity under hypoxic conditions. They used a new NMOF material (Mn-MOF) with Mn (II) as the active center, directly used to increase O<sub>2</sub> levels, and simultaneously applied to enhance PDT to produce ROS. Both

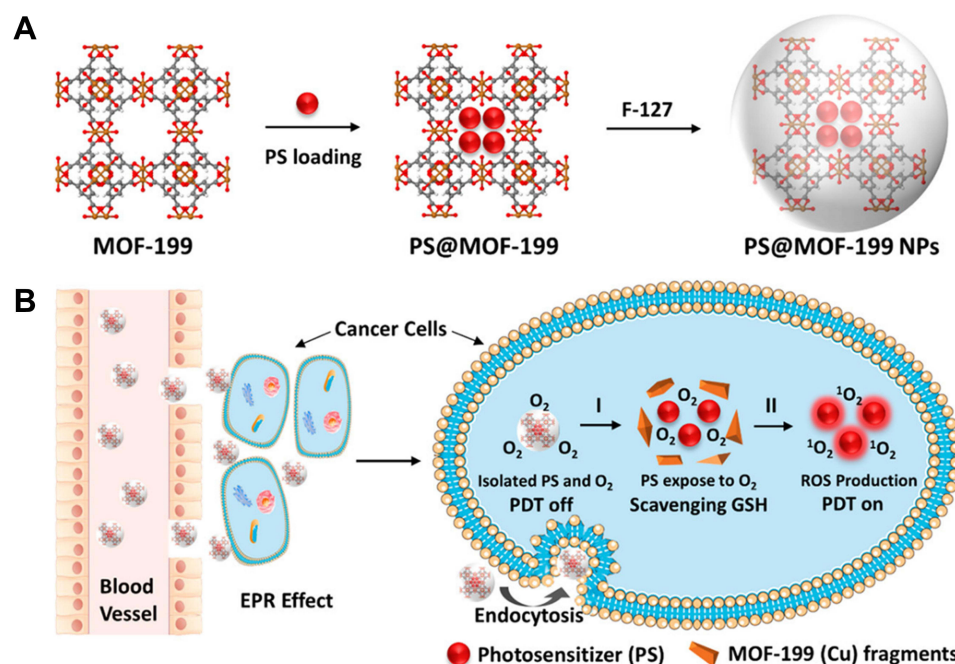


**Figure 9 (A)** Synthetic scheme to PS@MOF-199 and F127-coated PS@MOF-199 (PS@MOF-199 NPs); **(B)** quench and trigger of photosensitization originated from PS@MOF-199 NPs in the tumor microenvironment. Reprinted with permission from Wang Y, Wu W, Liu J et al. Cancer-Cell-Activated Photodynamic Therapy Assisted by Cu(II)-Based Metal-Organic Framework. *ACS Nano*. 2019;13(6):6879–6890. Copyright (2019) American Chemical Society.<sup>106</sup>

in vivo and in vitro experiments had proved that Mn-MOF increased the level of O<sub>2</sub> in tumors and further improved the efficiency of PDT.

### Other Active MOFs

Zhao et al<sup>109</sup> used MOFs, whose organic ligand was imidazole containing disulfide and the metal ions were Zn<sup>2+</sup>, physically loaded with Ce6 (Figure 10). This MOF decomposed in acidic organelles while promoting escape through the proton sponge effect caused by imidazole band ionization. Regardless of light irradiation, Ce6-loaded nanocarriers caused the consumption of intracellular GSH through the disulfide bond-thiol exchange reaction in 4T1 cells. GSH consumption would further lead to inactivation of glutathione peroxidase 4 (GPX4) and further enhanced cytotoxicity. The in vivo antitumor efficacy of all-active nanocarrier was demonstrated in a 4T1 tumor-bearing mouse model. Due to the combination of ferroptosis inhibitor and iron chelator, the antitumor effect of nanocarrier was weakened. This work indicated the effect of ferroptosis caused by all-active MOF on antitumor PDT.

### Inactive MOFs

PDT reagents based on MOFs can also be prepared by PSs and inactive MOFs, and the PSs bound by MOFs can also be not limited to porphyrins and their derivatives. MOFs as the carriers are undoubtedly an excellent method. Compared with other carriers, MOFs as the carrier shows great advantages: The porosity of MOFs endows them with high drug loading; furthermore, the stable crystal structure of MOFs allows the integration of a large number of PSs to generate cytotoxic ROS under light irradiation, which contributes to cytotoxic effects on cancer cells.

### PS Loading

The advantages of MOFs for PSs loading are: 1) the pores of MOFs limit the cargo in the pores, preventing it from interacting with oxygen before reaching the tumor area, resulting in better stability; 2) the special structure of MOFs isolates PSs well, which prevents the self-aggregation and self-quenching of PSs, and the generated substances are easy to diffuse, thus improving ROS generation.

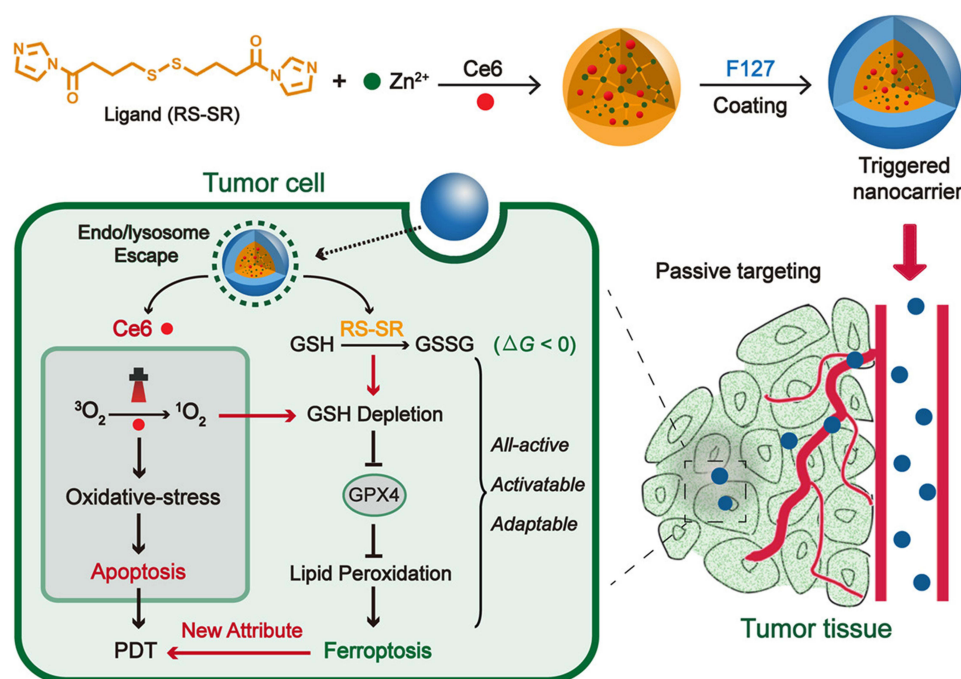


**Figure 10** Schematic illustration of all-active MOF nanocarriers for antitumor PDT that involves both apoptosis and ferroptosis. Reprinted with permission from Meng X, Deng J, Liu F et al. Triggered All-Active Metal Organic Framework: Ferroptosis Machinery Contributes to the Apoptotic Photodynamic Antitumor Therapy. *Nano Lett.* 2019;19(11):7866–7876. Copyright (2019) American Chemical Society.<sup>109</sup>

General PSs loading has two ways: 1) loading PSs after composing MOFs;<sup>25</sup> 2) loading during composing MOFs.<sup>110</sup> Zhang et al<sup>36</sup> encapsulated ultrasmall size gold nanoclusters (AuNCs) as photosensitizers in MOF ZIF-8 and further loaded DOX to obtain pH-responsive nanoprobes (AuNCs@MOF-DOX). Under acidic conditions in TME, the stable structure of ZIF-8 was destroyed, which accelerated the release of AuNCs and DOX, and improved the therapeutic effect of PDT/CD. Sometimes MOFs are more than just efficient carriers. Wang et al<sup>111</sup> used Cu (II)-based MOF (MOF-199) as an inert carrier to load PS precursors to achieve efficient delivery, and also as a Cu (I) catalyst source for in-situ click reaction to form PSs in tumor cells. In-situ synthesized PSs targeting mitochondria ultimately implement accurate photodynamic therapy.

## PS Surface Connection

Not only can PSs be mounted in MOFs, but also can be connected to MOFs. There are two common joining methods: covalent joining and non-covalent joining that is usually carried out after the synthesis of MOFs. The ideal PS connection is irreversible, avoiding the risk of early leakage. Kan et al<sup>112</sup> chose S-ethylthiol ester monosubstituted porphyrin molecules (TPP-SH) to be the post-synthesis reagent (Figure 11A). Under mild conditions, TPP-SH and UiO-66 NMOF were synthesized to form a surface decorative porphyrin MOF (UiO-66-TPP-SH) with a size less than 150nm by post-synthesis method (Figure 11B). This MOF with surface decorative porphyrin could not only maintain crystallinity, structural characteristics, and the size of the original UiO-66 NMOF (Figure 11C and D), but also efficiently generated  $^1\text{O}_2$  for improving the PDT effect. In addition, it had low cytotoxicity, high photocatalytic efficiency as well as good membrane permeability (Figure 11E and F). UiO-66-TPP-SH showed significantly higher photodynamic activity and more effective tumor therapy of PDT, compared to previous internal-located porphyrinic MOF.

Besides modified groups, some biomacromolecules, such as DNA, can also act as linkers to connect PSs with MOFs. Meng et al<sup>55</sup> prepared aptamer-functionalized Zr-MOFs consisting of  $\text{Zr}^{4+}$  and  $\text{H}_2\text{BDC}$  for targeted bioimaging and targeted PDT. The synthesized DNA containing an aptamer and a guanine-rich DNA segment formed a G-quadruplex DNA structure (denoted as G4-aptamer) which was a carrier to load the PS (denoted as TMPyP4) and specifically recognized target cells. Based on the strong binding capacity between phosphate-functionalized aptamers and Zr-MOFs

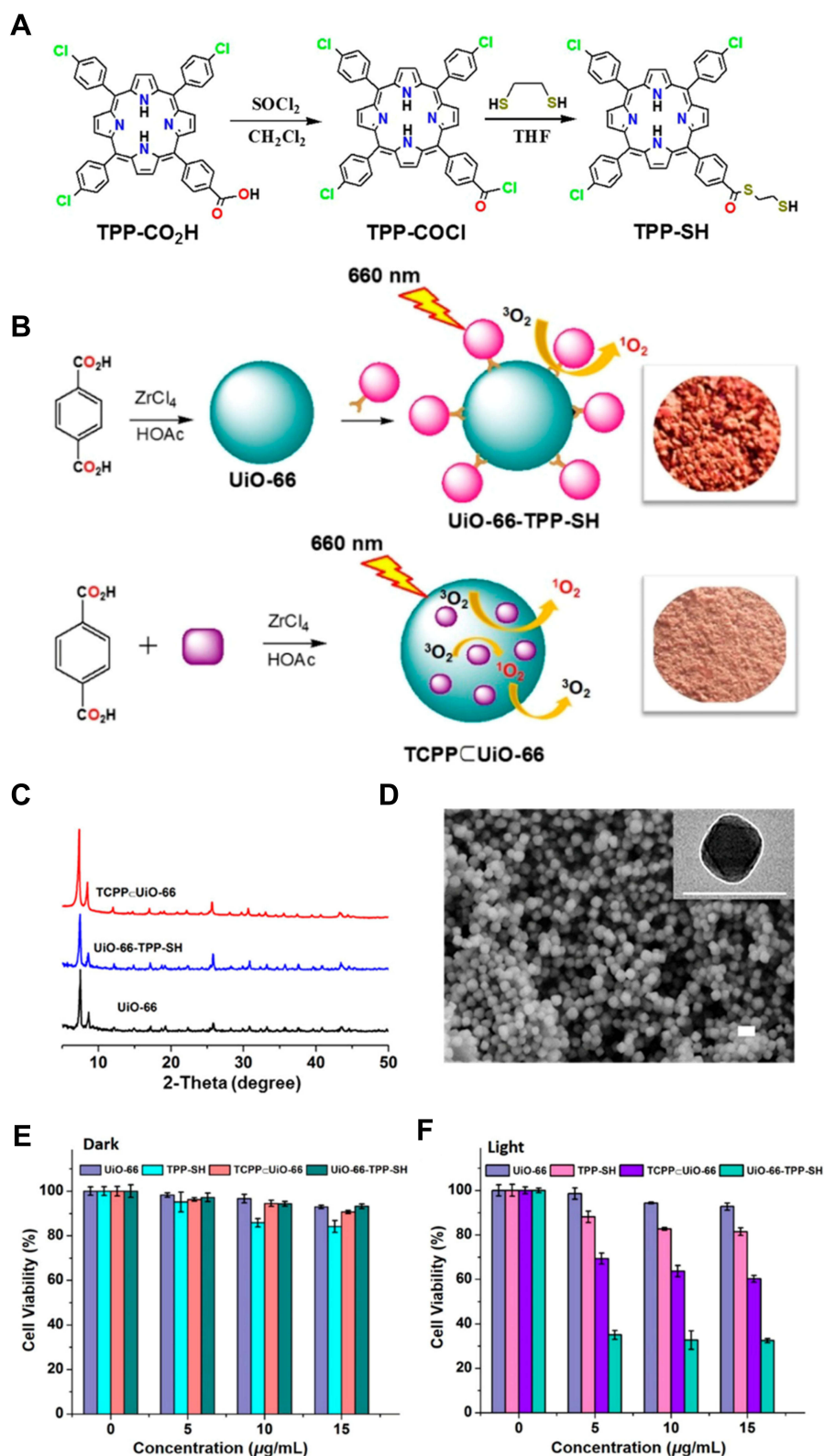


**Figure 11** The synthesis process of TPP-SH (A); UiO-66-TPP-SH and TCPP@UiO-66 (B); (C) PXRD Figure of UiO-66, TCPP@UiO-66, and UiO-66-TPP-SH; (D) SEM and TEM (inset) images of UiO-66-TPP-SH. Scale bar is 200 nm; In vitro cytotoxicity of UiO-66, TPP-SH, TCPP@UiO-66, and UiO-66-TPP-SH without (E) and with (F) light irradiation. Reprinted with permission from Kan JL, Jiang Y, Xue A et al. Surface Decorated Porphyrinic Nanoscale Metal-Organic Framework for Photodynamic Therapy. *Inorganic chemistry*. 2018;57(9):5420–5428. Copyright (2018) American Chemical Society.<sup>112</sup>



(Zr-O-P bonds), as well as the embedding of photosensitizer TmPyp4 in the G-quadruplex DNA structure, the G4-aptamer was easily united to TMPyP4 and Zr-NMOFs to form TMPyP4-G4-aptamer-NMOFs. Once the nanoplatform was delivered into cancer cells via the guiding aptamer, upon the light irradiation, the TMPyP4 was activated, generating sufficient ROS to efficiently kill cancer cells. It was studied that the specific recognition ability and phototoxicity of TMPyP4-G4-aptamer-NMOFs in vitro stability. For in vivo experiments, nanosystems were injected into a mouse model of subcutaneous xenograft HeLa tumors. The nanosystem resulted in 90% cell death of targeted cancer cells. The experimental results showed that the proposed nanosystem could selectively bind to target cells and act as a PS.

The connection between PSs and MOFs prevents premature leakage of PSs, moreover, improves the dispersion and stability of MOFs. For instance, Chen et al<sup>113</sup> modified and optimized NMOF (UiO-68-NH<sub>2</sub>) using protoporphyrin IX (PpIX) via controlling photoactive properties to realize combinational tumor PDT and PTT, which provided a utility method to provide a practical way to reduce monotherapy resistance, overcome adverse side effects and offer synergies to enhance their efficiency. Through the conjugated modification of PpIX on the surface of UiO-68-NH<sub>2</sub>, the dispersion and stability of the UiO-68-NH<sub>2</sub> particles were improved. After irradiation and activation of 635nm single wavelength light, nPCU NP could effectively transform the light energy, generate ROS and heat, and maintain the porosity of the UiO-68-NH<sub>2</sub> for further loading of other drugs. In vitro studies also proved that nPCU NP could be effectively absorbed by cells under the condition of simulating an anoxic environment in vivo, and it had good concealment ability for successful endosomal escape, showing enhanced phototherapeutic effect.

Guan et al<sup>114</sup> adopted a one-pot method to conduct in-situ self-assembly of imidazole-2-carboxaldehyde (IcaHs), Zn(NO<sub>3</sub>)<sub>2</sub>, and heavy atom iodine-attached Bodipy (2I-Bodipy) to synthesize a new PDT agent, 2I-BodipyPhNO<sub>2</sub>@ZIF-90 (Figure 12). 2I-BodipyPhNO<sub>2</sub>@ZIF-90 had an average diameter of <80 nm, and the introduction of 2I-BodipyPhNO<sub>2</sub> did

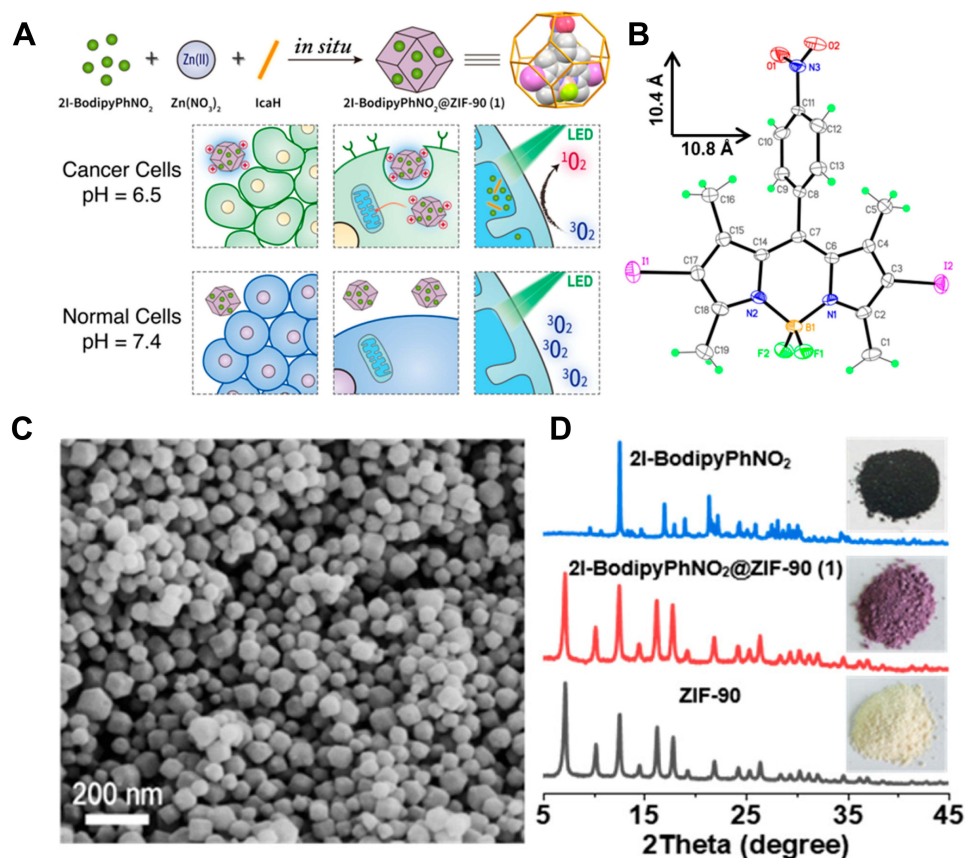


**Figure 12 (A)** The schematic illustration of the preparation of 1 and artistic representation of its pH-driven selective uptake of cancer and normal cells, and targeting of mitochondria under PDT; **(B)** perspective view of 2I-BodipyPhNO<sub>2</sub>; **(C)** SEM image of 1; **(D)** PXRD patterns of ZIF-90, 1, and 2I-BodipyPhNO<sub>2</sub>. The photographs of as-synthesized samples are shown in the inserts. Reprinted with permission from Guan Q, Zhou LL, Li YA, Dong YB. Diiodo-Bodipy-Encapsulated Nanoscale Metal-Organic Framework for pH-Driven Selective and Mitochondria Targeted Photodynamic Therapy. *Inorganic chemistry*. 2018;57(16):10,137–10,145. Copyright (2018) American Chemical Society.<sup>114</sup>

not affect the crystal lattice of ZIF-90, proving that the guests were enclosed in the framework. The 2I-Bodipy dyes were covalently linked to periodically arrange in the frame of ZIF-90 MOF, which effectively avoided their aggregation and self-quenching. The photosensitive system was characterized by low cytotoxicity, high cell permeability, good biocompatibility, pH-driven selective tumor cell uptake, mitochondrial targeting, and efficient  $^1\text{O}_2$  generation. Under the same conditions, it had higher antitumor efficacy and selectivity than free 2I-BodipyPhNO<sub>2</sub>, so it could be used as a highly effective new PDT agent to improve the efficacy of antitumor therapy.

## Integration for Optimizing Antitumor Effect

PDT has confirmed the potential to treat cancers, but only using PDT has a narrow effect for in vivo therapy, especially in large and deep tumor tissues.<sup>115</sup> At present, it is the mainstream to further optimize the overall antitumor effect of PDT by integrating with the advantages of MOFs-based PDT and other technologies.

## Targeting Tumor Microenvironment

In the process of PDT, there are some major constraints on its antitumor efficiency. On the one hand, hypoxic conditions in TME cannot provide continuous support for ROS production. On the other hand, the highly active ROS produced is easy for quenching, having a short half-life. Meanwhile, the GSH in the environment will also consume ROS. These would result in low ROS utilization efficiency and thus affecting the effect of PDT treatment.

### Relieve TME Hypoxia

As we all know, TME is hypoxic and acidic.<sup>116</sup> However, PDT is an oxygen-dependent antitumor therapy. Hence, PDT cannot efficiently utilize oxygen in TME leading to a significant reduction in PDT efficacy. In addition, hypoxia promotes angiogenesis and aggravates hypoxia, ultimately promoting tumor immune escape.<sup>117</sup> Therefore, effective oxygen supplementation in the TME site is very important.

Most researchers have prepared composites by combining MOFs with other oxygenating materials properly to improve PDT.<sup>75</sup> The porous structure of MOF can provide a suitable room for loading these oxygenating materials without compromising their functions. For instance, Sun et al<sup>56</sup> designed and constructed a novel MOF-based drug delivery system (BSA-MnO<sub>2</sub>/Ce6@ZIF-8) to resolve the difficulty in the effective aggregation of hydrophobic Ce6 in tumor areas. Ce6@ZIF-8 was prepared by one-pot synthesis, and the Ce6 was loaded inside the ZIF-8 (Figure 13A). This ZIF-8 was exploited to be a “separation chamber” that loaded and delivered Ce6, improving its dissolubility in the aqueous environment. The special structure of ZIF-8 could also efficiently keep the Ce6 isolated and avoid self-aggregate. Meanwhile, the drug loading capacity of Ce6 in ZIF-8 was high up to 28.3 wt %, which contributed to the effective aggregation of Ce6 in tumor cells. The bovine serum albumin (BSA)-MnO<sub>2</sub> NPs with a catalase-like activity gave this system the capacity to the self-sufficiency of O<sub>2</sub>, which helped alleviate hypoxia in the TME. When irradiated by 650 nm light with a low power density (230 mW/cm<sup>2</sup>), this system could be able to generate  $^1\text{O}_2$  leading to apoptotic and necrotic (Figure 13B and C).

Other researchers have tried to design MOF as enzyme with a catalase-like activity that catalyzes excess H<sub>2</sub>O<sub>2</sub> to O<sub>2</sub> in the TME.<sup>25,118,119</sup> Zhao's group<sup>57</sup> reported that a multifunctional mesoporous nanoenzyme (NE) derived from MOFs, namely MCOPP-NE (Figure 14A), was used to generate endogenous O<sub>2</sub> (Figure 14B and C) and improve the antitumor efficacy of PDT. The NE was prepared by simple annealing of Mn-based MOFs coated with mesoporous silica at room temperature, and then it was then modified with polydopamine and polyethylene glycol to improve its biocompatibility. Meanwhile, Ce6, a common PS, was loaded on the NE. After the catalytic reaction of MCOPP-NE with endogenous H<sub>2</sub>O<sub>2</sub> to O<sub>2</sub>, the hypoxia condition was alleviated. In vivo and in vitro experiments proved that the catalytic reaction of NE could alleviate the hypoxia condition (Figure 14D–G). Additionally, MCOPP-NE had a high loading capacity on Ce6, and the prepared MCOPP-NE-Ce6 could significantly improve the therapeutic effect of PDT on hypoxic tumors (Figure 14H).

### Reduce GSH

High GSH in TME is unfriendly to ROS generated by PDT, which reduces the antitumor efficacy of PDT. Therefore, increasing ROS production can be achieved by decreasing the level of intracellular GSH.<sup>120</sup>



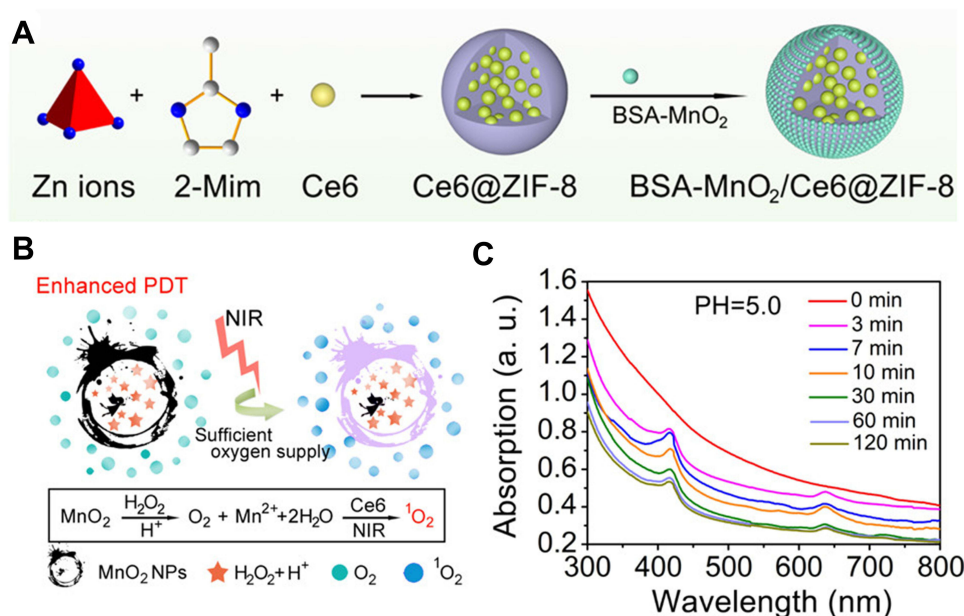


**Figure 13** (A) Schematic Illustration for the Formation of a BSA-MnO<sub>2</sub>/Ce6@ZIF-8 nanoplateform and (B) degradation behavior of BSA-MnO<sub>2</sub>/Ce6@ZIF-8 NPs dispersed in DI water with pH 5.0; (C) oxygen production ability of Ce6@ZIF-8 and BSA-MnO<sub>2</sub>/Ce6@ZIF-8 NPs dispersed in DI water with different pH in the presence of H<sub>2</sub>O<sub>2</sub>. Reprinted with permission from Sun Q, Bi H, Wang Z et al. O<sub>2</sub>-Generating Metal–Organic Framework-Based Hydrophobic Photosensitizer Delivery System for Enhanced Photodynamic Therapy. *ACS Applied Materials & Interfaces*. 2019;11(40):36,347–36,358. Copyright (2019) American Chemical Society.<sup>56</sup>

At present, there are few studies on the direct reduction of GSH in PDT. What is common is that Mn-based materials, such as manganese dioxide,<sup>121</sup> directly react with GSH in the redox reaction to reduce the level of GSH in cells. Zhou et al<sup>122</sup> used MnO<sub>2</sub> to improve the PDT effect of constructing a multifunctional nanoplateform. MnO<sub>2</sub> catalyzed H<sub>2</sub>O<sub>2</sub> to generate O<sub>2</sub> to relieve hypoxia and photodynamic sensitization while reducing GSH to resist tumor antioxidant defense. Xiao et al<sup>75</sup> further used MnO<sub>2</sub> for achieving magnetic resonance imaging (MRI). Mn<sup>2+</sup> in the solution showed excellent MRI capabilities. At the cellular level, due to the effective etching of the MnO<sub>2</sub> layer after endocytosis, the red fluorescence appeared after light excitation, confirming that Mn<sup>2+</sup> was able to achieve effective MRI imaging.

### Low pH

It is well known that the changes in metabolism in tumor cells result in low pH in TME. At this point, tumor cells preferentially utilize glycolysis as the main means of providing energy, which is called anaerobic glycolysis. This results in an increase in lactic acid in the extracellular environment and diffusion of H<sup>+</sup> into the intercellular stroma. Therefore, pH-sensitive MOFs are used to be delivery carriers for PSs that are specifically cleaved or protonated in an acidic environment to responsively release photosensitizers within tumor cells and thus exert antitumor efficacy. pH-sensitive MOFs ensure relative stability in a neutral physiological environment and accelerate release in an acidic tumor microenvironment. ZIF-8 has cleavage properties in TME. Yu et al<sup>110</sup> successfully encapsulated Ce6 into ZIF-8 (ZIF-8@Ce6) using a one-pot encapsulation and the self-assembly approach and subsequently modified HA (ZIF-8@Ce6–HA) to improve biocyclic properties and biocompatibility while targeting the CD44 receptor. The slow and weak release of Ce6 was observed at pH 7.4, while the release was accelerated in acidic solution (pH 5.5).

### Combination Therapy

To improve the overall antitumor efficacy, MOF-based PDT is often used in combination with various therapies (eg CT, RT, starvation therapy, immunotherapy, etc.). As shown in Table 2, combination therapy has both advantages and disadvantages compared to PDT alone.

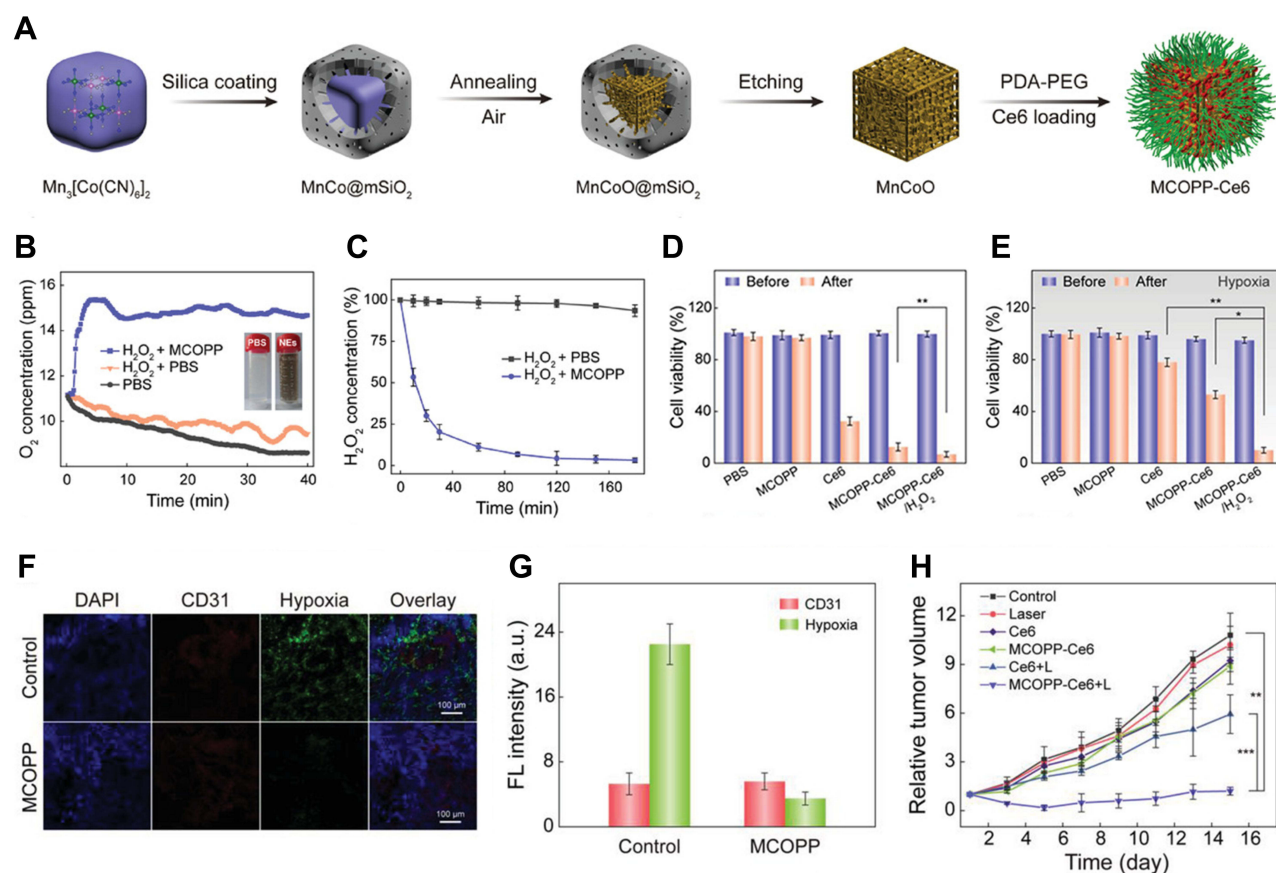


**Figure 14** (A) Representation of the preparation process of MCOPP NE; (B)  $O_2$  generation of MCOPP NE. The inset images show photographs of  $H_2O_2$  solutions with and without MCOPP NE; (C) degradation of  $H_2O_2$  with and without MCOPP NE. Cell viability of 4T1 cells treated in normoxic (D) and hypoxic (E) environments before and after 671 nm laser irradiation; (F) representative immunofluorescence images of tumor slices after hypoxia staining. The hypoxia areas and blood vessels were stained by anti-pimonidazole antibody (green) and anti-CD31 antibody (red); (G) relative hypoxia positive areas and blood vessel density measured by the Image J software; (H) relative tumor volume of mice after treatments (n = 5). Reprinted with permission from Wang D, Wu H, Lim WQ et al. A Mesoporous Nanoparticle Derived from Metal-Organic Frameworks with Endogenous Oxygen Generation to Alleviate Tumor Hypoxia for Significantly Enhanced Photodynamic Therapy. *Adv Mater.* 2019;31(27):e1901893. Copyright (2019) WILEY-VCH Verlag GmbH & Co. KGaA, Weinheim.<sup>57</sup>

## Combining PDT with CT

CT is a kind of treatment that uses anticancer chemical drugs to prevent proliferation, invasion, and metastasis of cancer cells and finally kills cancer cells, which is a systemic treatment method. At present, CT is still the main

**Table 2** The Advantages and Disadvantages of Combination Therapy Compared with PDT

Combination Therapy	Advantages	Disadvantages	Ref
PDT + CT	Improve safety of chemotherapy; avoid multi-drug resistance (MDR); improve overall antitumor efficacy	Unavoidable toxicity of chemotherapy drugs	[123–127]
PDT + RT	Achieve deep tumors therapy; increase the sensitivity of tumor to RD; achieve abscopal effect	Unavoidable side effects of RD	[128–131]
PDT + Starvation therapy	Amplify of therapeutic effect; suit for hypoxic tumors	Enzyme' shortcomings, such as poor stability, short half-life and immunogenicity; the systemic toxicity of $H_2O_2$	[49,132–135]
PDT + immunotherapy	Effectively inhibit tumor recurrence and metastasis; enhance antitumor immunity	An adverse reaction caused by an overactive immune system	[90,123,136,137]

clinical treatment method.<sup>138</sup> PDT itself has limitations in hypoxic tumors due to the lack of adequate oxygen in the TME. Combining CT with PDT could make up for the limitations of PDT in the treatment of hypoxic tumors.<sup>139</sup> Chemotherapy drugs including DOX,<sup>140</sup> oxaliplatin,<sup>141</sup> or gemcitabine<sup>142</sup> have been combined with PDT to implement antitumor combination therapy. Lee's group<sup>48</sup> first reported core-shell nanoparticles consisting of a PDT agent and a MOF shell with a chemotherapeutic agent for the combined treatment of PDT and CT. They used graphite-carbon nitride (g-C<sub>3</sub>N<sub>4</sub>) nanosheets as core and grew ZIF-8 on its surface to form g-C<sub>3</sub>N<sub>4</sub>@ZIF-8 core-shell NP. The g-C<sub>3</sub>N<sub>4</sub> nanosheet is an effective visible-light PS. Singlet oxygen was generated in the g-C<sub>3</sub>N<sub>4</sub> nanosheet upon the light irradiation, and it was effectively diffused through the ZIF-8 shell. Additionally, DOX was loaded into the ZIF-8 shell of g-C<sub>3</sub>N<sub>4</sub>@ZIF-8 NP. The red fluorescence of DOX and the blue fluorescence of g-C<sub>3</sub>N<sub>4</sub> nanosheets could effectively perform dual-color fluorescence imaging on tumor cells. Combining with CT efficacy of DOX and PDT efficacy of g-C<sub>3</sub>N<sub>4</sub> nanosheet could perform d imaging-guided photo-chemo therapy, and significantly improve the overall antitumor efficacy.

Since PDT is an oxygen-dependent treatment and TME is hypoxia, some hypoxia-activated chemotherapy drugs would be more effective in the hypoxic environment exacerbated by PDT. A combination therapy associating PDT with hypoxia-activated CT is ideal and complementary. Xie's group<sup>143</sup> synthesized a multifunctional Hf-porphyrin NMOF platform Hf/tetra (4-carboxyphenyl) porphine (TCPP) with more than 50wt% of TCPP, good crystallization, and a large Brunauer–Emmett–Teller surface for high loading of a hypoxia-activated prodrug tirapazamine (TPZ) up to 85.28 µg/mg. In addition, the surface modification of TPZ/Hf-TCPP with dopamine-derived polymer (DOPA-IMA-MPEG) could significantly improve the dispersion and stability of TPZ/Hf-TCPP, and achieve the controlled release of TPZ. TPZ/Hf-TCPP/PEG effectively produced ROS for PDT upon light irradiation. Meanwhile, the utilization of O<sub>2</sub> by PDT further intensified hypoxia, thus inducing the activation of TPZ, which had been verified to generate great cytotoxicity on both Hela and 4T1 cells. In vivo experiments on 4T1 tumor-bearing mice also confirmed that this combination therapy had the significant antitumor efficacy, compared with other single therapies (Figure 15).

### Combining PDT with RT

Although combining with PDT can reduce CT toxicity, the toxicity of chemotherapeutic drugs is still inevitable. RT is a clinic antitumor therapy that employs radiation such as X-rays to kill and destroy cancer cells.<sup>144</sup> PDT lacks widely clinical application mainly due to light penetration, and it is still a big challenge to achieve effective treatment of deep tumors. X-ray has strong tissue penetration, so combining PDT with RT is expected to inhibit deep tumor growth and achieve effective treatment of deep tumors. Liu et al<sup>145</sup> designed a novel MOF (Hf-TCPP MOF) composed of Hf<sup>4+</sup> and TCPP, in which Hf, one of the high-Z elements, could be used as a sensitizer for RT. Meanwhile, MOF was coated with polyethylene glycol (PEG) so that it played a role in tumor homing after intravenous injection. The combination of PDT and RT achieved a better antitumor effect in vivo. These nanoparticles had a high TCPP loading, which was conducive to the effective production of ROS under light exposure. Hf as a radiotherapy sensitizer absorbed ionizing radiation and improved the effect of radiotherapy. More importantly, the NMOF nanoparticles did not cause significant toxicity to the mice, and they could degrade and be excreted quickly.

### Combining PDT with Starvation Therapy

Starvation therapy, as its name suggests, starves tumor cells to death, blocking and cutting off the energy supply, and preventing them from using energy for reproducing and spreading. Glucose is the energy source of tumor cells. Tumor cells rely on anaerobic glycolysis to decompose glucose and provide energy for their growth.<sup>146</sup> In general, starvation therapy is achieved through glucose oxidase (GOX)<sup>147,148</sup> or bionic enzymes with a glucose-like activity that competes with tumor cells to utilize glucose, thus inhibiting the tumor growth. Recently, researchers have paid more and more attention to the combination of MOF-based PDT with starvation therapy. For instance, Li et al<sup>49</sup> adopted PCN-224 which was used as a PS and simultaneously as a nanocarrier to further load GOX and catalase and subsequently coated with a cancer cell membrane. The cascaded bioreactor

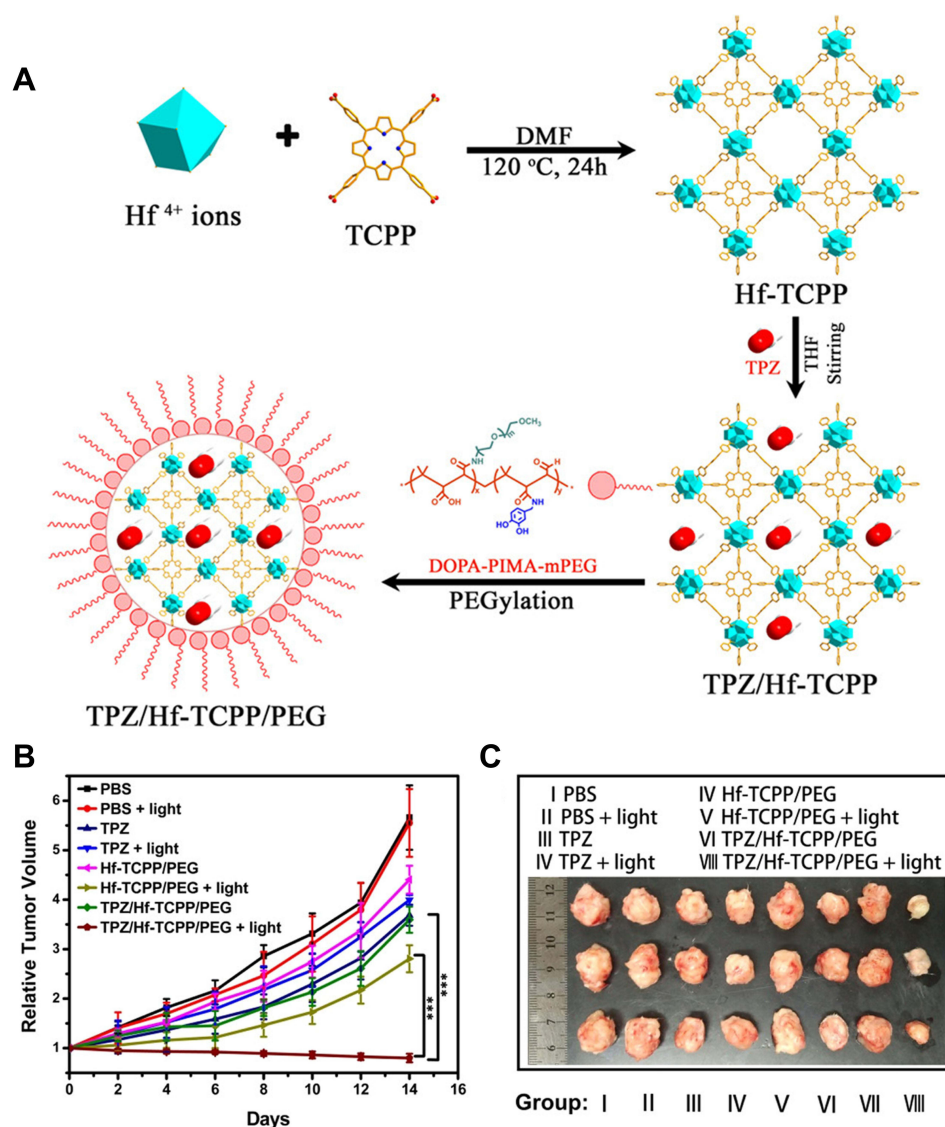


**Figure 15 (A)** The synthesis process of TPZ/Hf-TCPP/PEG; **(B)** time-dependent tumor growth curves via tail vein administration at a concentration of 5.0 mg/mL (200 μL); **(C)** tumor images obtained after different treatments for 14 days. Reprinted with permission from Liu M, Wang L, Zheng X, Liu S, Xie Z. Hypoxia-Triggered Nanoscale Metal-Organic Frameworks for Enhanced Anticancer Activity. *ACS Appl Mater Interfaces*. 2018;10(29):24,638–24,647. Copyright (2018) American Chemical Society.<sup>143</sup>

mem@catalase@GOx@PCN-224 (mCGP) was obtained (Figure 16A). The mCGP was constructed for cancer-targeted starvation therapy and PDT where PCN-224 ensured the smooth progression of the cascade reaction. Due to the ability of immune escape and homologous targeting given by the cancer cell membrane (Figure 16B), mCGP avoided premature clearance and effectively accumulated in the cancer tissue, thus improving the internalization efficiency of cancer cells. Under the light irradiation, the cascade reactions of mCGP boosted the catalysis of endogenous H<sub>2</sub>O<sub>2</sub> to produce O<sub>2</sub>, accelerated the decomposition of glucose, and increased the production of cytotoxic <sup>1</sup>O<sub>2</sub> (Figure 16C). This cascade provided a steady supply of oxygen to regulate the tumor's anoxic microenvironment, thereby producing more cytotoxic <sup>1</sup>O<sub>2</sub> while inhibiting the anoxic glycolysis response of tumor cells to glucose and reducing the energy supply of tumor cells (Figure 16D–F). This cascaded bioreactor further accelerated the efficacy of antitumor therapy by synergizing starvation therapy with PDT. Therefore, this work demonstrated that the combination of long-term starvation therapy and powerfully robust PDT would amplify the antitumor effect and more effectively inhibit tumor development in a spatiotemporally controlled manner.



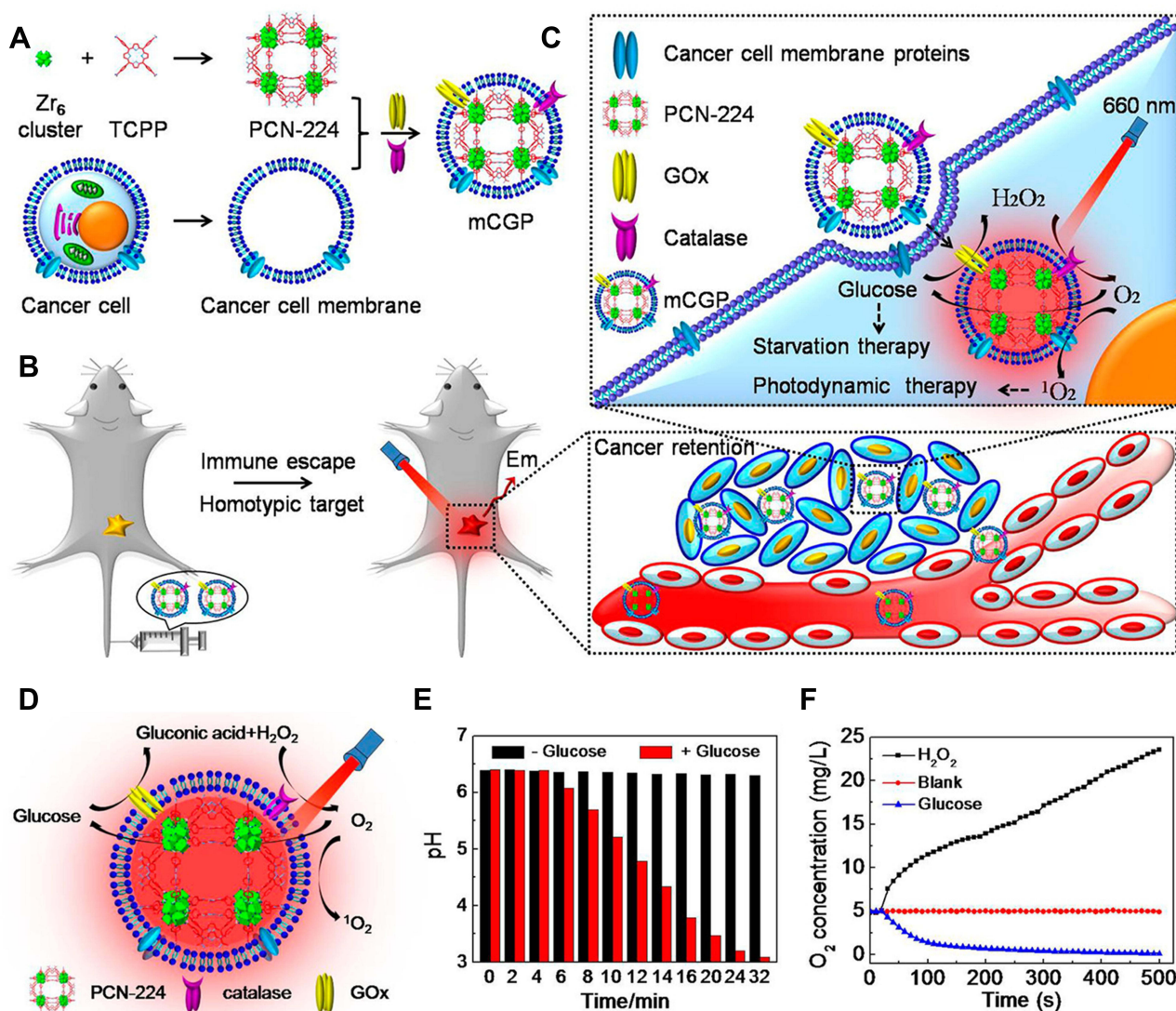


**Figure 16** (A) The synthetic process for mCGP; (B) the immune escape and homotypic targeting abilities of mCGP; (C) the cascade reactions amplify the synergistic effects of mCGP for starvation therapy and PDT; (D) schematic illustration of the cascade reactions of mCGP including catalyzing the breakdown of  $H_2O_2$ , decomposing glucose, and producing  $^1O_2$ ; (E) the pH value changes of mCGP solution in the absence and presence of glucose; (F) the  $O_2$  concentration changes of mCGP solution in the presence of  $H_2O_2$  or glucose. Reprinted with permission from Li SY, Cheng H, Xie BR et al. Cancer Cell Membrane Camouflaged Cascade Bioreactor for Cancer Targeted Starvation and Photodynamic Therapy. *ACS Nano*. 2017;11(7):7006–7018. Copyright (2017) American Chemical Society.<sup>49</sup>

Since bionic enzymes have high catalytic activity as enzymes and have good adaptability.<sup>118,119</sup> Liu et al<sup>80</sup> applied Pt NPs with catalase-like activity and aurum (Au) NPs with GOX-like activity to set off a cascade catalytic reaction for combined PDT and starvation therapy. The polyvinylpyrrolidone (PVP)-coated Pt NPs were attached to the surface of the prepared PCN and wrapped by another PCN shell, forming a sandwich structure (P@Pt@P) supported by MOFs. Due to the porous structure of PCN, in situ generation of Au NPs could be embedded in the channel, and the channel restricted and stabilized Au NPs. FA was introduced on the surface of the prepared nanoparticles (P@Pt@P-Au) to improve their stability in vivo. By oxidizing  $H_2O_2$  inside the tumor to  $O_2$ , Pt NPs effectively relieved the hypoxia inside the tumor and enhanced the therapeutic effect of oxygen-dependent PDT. The generated oxygen subsequently would also improve the utilization of glucose by Au NPs to deplete the glucose needed for the survival of tumor cells. This cascade catalytic reaction was complementary to each other to implement the synergistic effect of PDT combined with starvation therapy to further enhanced antitumor therapy and prevented metastasis and recurrence (Figure 17).

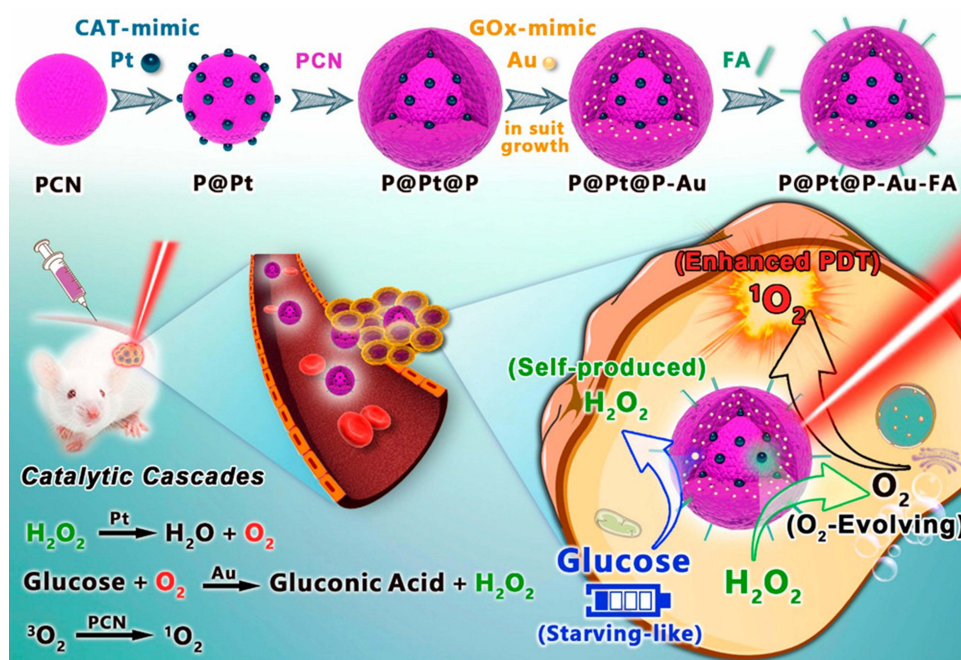


**Figure 17** The schematic diagram of synergistic cancer treatment by catalytic cascade enhancement of porphyrin MOF (PCNs)<sup>a</sup> with double inorganic nanoenzyme engineering. Reprinted with permission from Liu C, Xing J, Akakuru OU et al. Nanozymes-Engineered Metal-Organic Frameworks for Catalytic Cascades-Enhanced Synergistic Cancer Therapy. *Nano Lett.* 2019;19(8):5674–5682. Copyright (2019) American Chemical Society.<sup>80</sup>

### Combining PDT with Immunotherapy

Immune checkpoint blockade (ICB), one of immunotherapy, is an emerging antitumor therapy<sup>149</sup> that has received soaring attention with the successful launch of immune checkpoint inhibitors (Yervoy<sup>®</sup>, the first CTLA-4 inhibitor, and Opdivo, the first PD-1/PD-L1 inhibitor<sup>150</sup>). MOF-based PDT primes immunotherapy for ICD to increase the immune response rates, which has the potential to be addressing inherently complex problems in cancer treatment. Lan et al<sup>151</sup> designed a novel nMOF-based nPS, Fe-TBP, to overcome hypoxia and implement a synergistic combination of PDT and ICB whose purpose was to improve body immune response and prime non-inflamed tumors for anticancer therapy. Fe-TBP consisted of  $\text{Fe}_3\text{O}_4$  clusters and TBP ligands. When Fe-TBP is irradiated, the cascade reaction occurred, that was, the  $\text{Fe}_3\text{O}_4$  cluster decomposed endogenous  $\text{H}_2\text{O}_2$  to generate  $\text{O}_2$  through the Fenton-like reaction, and at the same time, the photo-excited porphyrins converted the generated  $\text{O}_2$  to cytotoxic  $^1\text{O}_2$ . In a mouse model of colorectal cancer, Fe-TBP mediated PDT elicited a systemic antitumor response that induced significant tumor infiltration of both  $\text{CD4}^+$  and  $\text{CD8}^+$  cytotoxic T cells, and subsequently significantly improved the therapeutic efficacy of  $\alpha$ -PD-L1 ICB, leading to 90% tumor regression in both primary and distant tumors.

Based on PDT and TPZ, Shao et al<sup>152</sup> also combined immunotherapy and rationally designed core-shell upconversion nanoparticle (UCNP) @ porphyrinic MOFs (UCSs) via the growth of porphyrinic MOFs on CA-modified UCNP for hypoxic tumors treatment. The UCNP core absorbed NIR light and efficiently transferred energy to the MOF shell, which was enabled to form NIR-triggered cytotoxic substances. Loading TPZ into the MOF shell was to obtain TPZ/UCSs. Experiments revealed that the combination of NIR-induced PDT and hypoxic-activated CD was expected to improve tumor treatment in vivo and in vitro. In addition, combined PDT-CD induced effective antitumor immunity, so its integration with anti-programmed death ligand 1 ( $\alpha$ -PD-L1)-guided immunotherapy further promoted specific infiltration of cytotoxic T cells, thereby completely inhibiting distant tumor development (Figure 18).



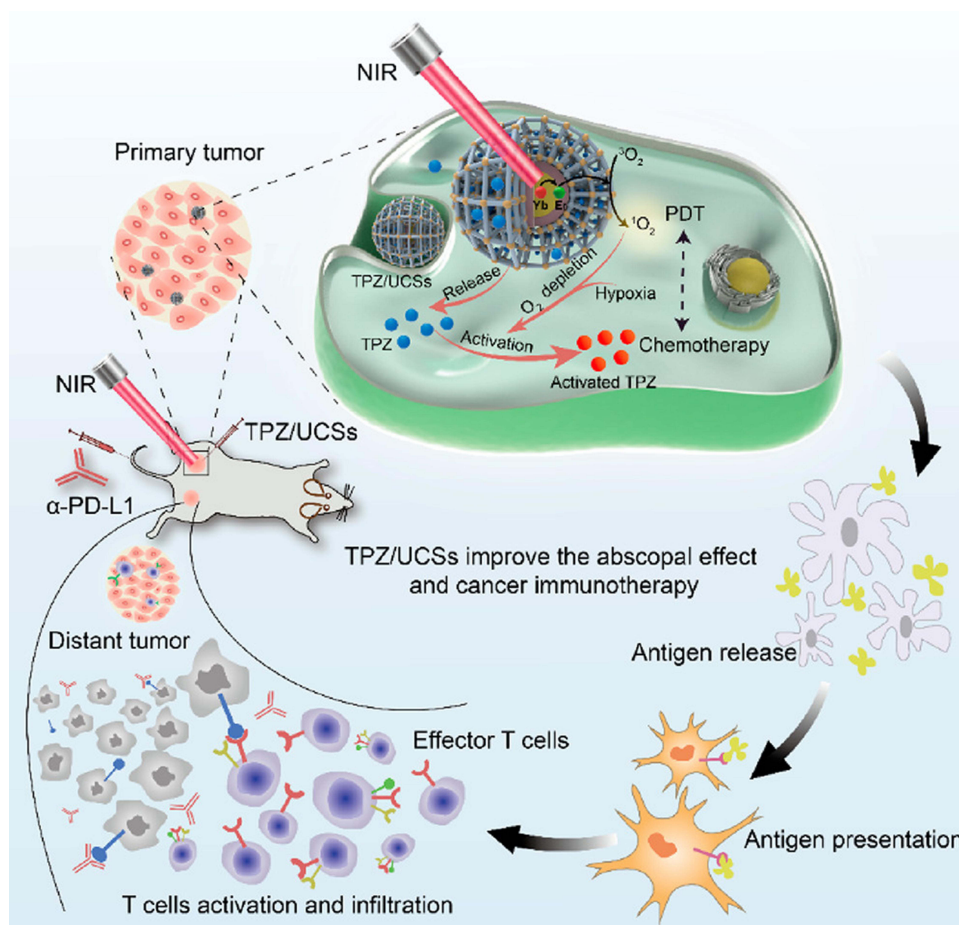


**Figure 18** The schematic diagram of TPZ/UCSs and their application to cancer treatment via NIR light-triggered PDT and hypoxia-activated chemotherapy with immunotherapy. Reprinted with permission from Shao Y, Liu B, Di Z et al. Engineering of Upconverted Metal-Organic Frameworks for Near-Infrared Light-Triggered Combinational Photodynamic/Chemo-/Immunotherapy against Hypoxic Tumors. *J Am Chem Soc.* 2020;142(8):3939–3946. Copyright (2020) American Chemical Society.<sup>152</sup>

## Conclusion and Outlook

MOF as a special material, which combines the advantages of organic materials and inorganic materials, has a wide range in gas adsorption, storage, and separation, catalysis, as well as in biomedical applications, especially in PDT. Currently, the most used MOFs for PDT are UiO-66 of the UiO series, ZIF-8 of the ZIF series, and the PCN-224 of PCN series (Table 3). Researchers have designed many new MOFs for PDT in the past two decades. On the one hand, developing inactive MOFs as low-toxic and high drug-loading carriers is to deliver more PSs to tumor tissues. On the other hand, designing active MOFs with certain functions is aim for increasing the accumulation of PSs in target tissues, as well as assisting PDT to enhance the therapy efficacy. Currently, the most used MOFs for PDT are UiO-66 of the UiO family, ZIF-8 of the ZIF family, and PCN-224 of the PCN family (Table 3). However, the research on MOFs-based photodynamic therapy mainly focuses on the function of MOFs-based synthetic nanosystems and the ultimate antitumor efficacy. The problems affecting the clinical development of MOFs-based PDT have been ignored, such as poor stability, low repeatability, and poor water dispersion. As the above problems are solved, more new types of MOFs will enter the biomedical application field and even enter the clinical field.

**Table 3** A Summary of MOFs for PDT Applications and Their Advantages

	Metal Center	Organic Ligands	Advantages	Ref.
DBP-UiO	Hf	H <sub>2</sub> DBP	High PS loading; more ROS production; enhanced ISC	[47]
DBC-UiO	Hf	H <sub>2</sub> DBC	High PS loading; high stability; high porosity; enhanced ISCs and more efficient <sup>1</sup> O <sub>2</sub> generation	[52]
Hf-TCPP	Hf	TCPP	High PS loading; large Brunauer–Emmett–Teller (BET) surface; RT sensitizer (Hf);	[143,145]
PCN-224	Zr		Improved chemical stability;	[49,54,88]
Zr-TBB	Zr	H <sub>4</sub> TBB	Achieve excellent photostability; perform type I and type II PDT; produce 4 types of ROS	[54]
PCN-229	Zr	H <sub>4</sub> TCP-2	Higher porosity and BET surface area	[76]
PCN-300	Zr	H <sub>4</sub> TCP-3	Excellent stability in aqueous solution with pH ranging from 0 to 12	[76]
TBP-MOF	Zr	H <sub>4</sub> TBP	Higher chemical stability; red-shifted absorption bands and stronger infrared luminescence characteristics	[90]
UiO-PDT	Zr	I <sub>2</sub> -BDP	Low dark toxicity; high cell uptake; good biocompatibility and high <sup>1</sup> O <sub>2</sub> production	[98]
UiO-68-NH <sub>2</sub>	Zr	2-aminoterephthalic acid	The amino group of the ligands provides the site for conjugate modification	[113]
UiO-66	Zn	Purified terephthalic acid (TPA)	Achieve nanosized porphyrin with heavy iodine atoms; achieve nanoscale; easy surface modification; high structural stability	[98,112]
ZIF-8	Zn	2-methylimidazole	pH-responsive property; easy to achieve nanoscale under mild synthesis conditions; good solubility in aqueous solution	[36,48,56,110]
ZIF-90	Zn	IcaHs; 2l-Bodipy	Avoid PS aggregation and self-quenching; low cytotoxicity; high cell permeability; good biocompatibility; pH-driven selective tumor cell uptake; mitochondrial targeting and efficient <sup>1</sup> O <sub>2</sub> generation	[114]
CuTz-I	Cu	3,5-diphenyltriazole (3,5-Ph <sub>2</sub> -tzH)	Carry oxygen, alleviate hypoxia; achieve type I PDT	[100]
MOF-199	Cu	H <sub>3</sub> BTC	Inert carrier; remove intracellular GSH	[106,111]
MOF-2	Cu;Al	Meso-tetrakis (4-carboxyphenyl) porphyrin	Decrease intracellular GSH	[105]
Ti-TBP	Ti	H <sub>4</sub> TBP	Produce 4 types of ROS; achieve hypoxia-tolerant type I PDT and oxygen-dependent type II PDT	[53]
Fe-TBP	Fe	H <sub>4</sub> TBP	Generate O <sub>2</sub> through Fenton-like reaction to overcome hypoxia	[151]

## Abbreviations

PDT, Photodynamic therapy; PSs, Photosensitizers; MOF, Metal-organic framework; TME, Tumor microenvironment; ROS, Reactive oxygen species; PEI, Polyethylene imine; NMOFs, Nanoscale metal-organic frameworks; ZIF, Zeolitic imidazolate framework; UiO, University of Oslo; PCN, Porous coordination network; ISCs, Intersystem crossings; CT, Chemotherapy; RT, Radiotherapy; TGI, Tumor growth inhibition; DOX, Doxorubicin; MIL, Materials of Institute Lavoisier; GSH, glutathione; ICD, Immunogenic cell death; FA, Folic acid; HA, Hyaluronic acid; Pt NPs, Platinum nanoparticles; SBUs, Secondary building units; SALE, Solvent-assisted ligand exchange; NIR, Near-infrared; CPT, Camptothecin; GPX4, Glutathione peroxidase 4; AuNCs, Gold nanoclusters; TPP-SH, S-ethylthiol ester monosubstituted porphyrin molecule; PpIX, Protoporphyrin IX; BSA, Bovine serum albumin; NE, Nanoenzyme; MRI, magnetic resonance imaging; MDR, Multi-drug resistance; TPZ, Tirapazamine; PEG, Polyethylene glycol; GOX, Glucose oxidase; PVP, Polyvinylpyrrolidone; ICB, Immune checkpoint blockade; UCNP, Upconversion nanoparticle; α-PD-L1, Anti-programmed death ligand 1; BET, Brunauer-Emmett-Teller; TPA, Terephthalic acid.

## Acknowledgments

This work was financially supported by National Natural Science Foundation of China (No. 32171362) and Natural Science Foundation of Shandong Province (No. ZR2021MH087).

## Disclosure

The authors report no conflicts of interest in this work.

## References

1. Dolmans DE, Fukumura D, Jain RK. Photodynamic therapy for cancer. *Nat Rev Cancer*. 2003;3(5):380–387. doi:10.1038/nrc1071
2. Stables GI, Ash DV. Photodynamic therapy. *Cancer Treat Rev*. 1995;21(4):311–323. doi:10.1016/0305-7372(95)
3. Manyak MJ, Russo A, Smith PD, Glatstein E. Photodynamic therapy. *J Clin Oncol*. 1988;6(2):380–391. doi:10.1200/jco.1988.6.2.380
4. Zhen X, Cheng P, Pu K. Recent Advances in Cell Membrane-Camouflaged Nanoparticles for Cancer Phototherapy. *Small*. 2019;15(1):e1804105. doi:10.1002/sml.201804105
5. Perlman SG, Gerber LH, Roberts RM, Nigra TP, Barth WF. Photochemotherapy and psoriatic arthritis. A prospective study. *Ann Intern Med*. 1979;91(5):717–722. doi:10.7326/0003-4819-91-5-717
6. Huang R, Zhang C, Bu Y, et al. A multifunctional nano-therapeutic platform based on octahedral yolk-shell Au NR@CuS: photothermal/photodynamic and targeted drug delivery tri-combined therapy for rheumatoid arthritis. *Biomaterials*. 2021;277:121088. doi:10.1016/j.biomaterials.2021.121088
7. van Dijk EHC, Fauser S, Breukink MB, et al. Half-Dose Photodynamic Therapy versus High-Density Subthreshold Micropulse Laser Treatment in Patients with Chronic Central Serous Chorioretinopathy: the PLACE Trial. *Ophthalmology*. 2018;125(10):1547–1555. doi:10.1016/j.ophtha.2018.04.021
8. Dong Y, Cao W, Cao J. Treatment of rheumatoid arthritis by phototherapy: advances and perspectives. *Nanoscale*. 2021;13(35):14591–14608. doi:10.1039/d1nr03623h
9. Nam J, Son S, Ochyl LJ, Kuai R, Schwendeman A, Moon JJ. Chemo-photothermal therapy combination elicits anti-tumor immunity against advanced metastatic cancer. *Nat Commun*. 2018;9(1):1074. doi:10.1038/s41467-018-03473-9
10. Liang X, Chen M, Bhattacharai P, Hameed S, Dai Z. Perfluorocarbon@Porphyrin Nanoparticles for Tumor Hypoxia Relief to Enhance Photodynamic Therapy against Liver Metastasis of Colon Cancer. *ACS Nano*. 2020;14(10):13569–13583. doi:10.1021/acsnano.0c05617
11. Donohoe C, Senge MO, Arnaut LG, Gomes-da-Silva LC. Cell death in photodynamic therapy: from oxidative stress to anti-tumor immunity. *Biochimica Et Biophysica Acta Reviews Cancer*. 2019;1872(2):188308. doi:10.1016/j.bbcan.2019.07.003
12. Fang J, Nakamura H, Iyer AK. Tumor-targeted induction of oxystress for cancer therapy. *J Drug Target*. 2007;15(7–8):475–486. doi:10.1080/10611860701498286
13. Chilakamarthi U, Giribabu L. Photodynamic Therapy: past, Present and Future. *Chemical Record*. 2017;17(8):775–802. doi:10.1002/tcr.201600121
14. Allison RR, Downie GH, Cuenca R, Hu XH, Childs CJ, Sibata CH. Photosensitizers in clinical PDT. *Photodiagnosis Photodyn Ther*. 2004;1(1):27–42. doi:10.1016/s1572-1000(04)
15. Ethirajan M, Chen Y, Joshi P, Pandey RK. The role of porphyrin chemistry in tumor imaging and photodynamic therapy. *Chem Soc Rev*. 2011;40(1):340–362. doi:10.1039/b915149b
16. Staron J, Boron B, Karcz D, Szczygiel M, Fiedor L. Recent Progress in Chemical Modifications of Chlorophylls and Bacteriochlorophylls for the Applications in Photodynamic Therapy. *Curr Med Chem*. 2015;22(26):3054–3074. doi:10.2174/0929867322666150818104034
17. Li L, Shao C, Liu T, et al. An NIR-II-Emissive Photosensitizer for Hypoxia-Tolerant Photodynamic Theranostics. *Adv Mater*. 2020;32(45):e2003471. doi:10.1002/adma.202003471
18. Farokhzad OC, Langer R. Impact of nanotechnology on drug delivery. *ACS Nano*. 2009;3(1):16–20. doi:10.1021/nn900002m
19. Hossen S, Hossain MK, Basher MK, Mia MNH, Rahman MT, Uddin MJ. Smart nanocarrier-based drug delivery systems for cancer therapy and toxicity studies: a review. *J Adv Res*. 2019;15:1–18. doi:10.1016/j.jare.2018.06.005
20. Chen W, Goldys EM, Deng W. Light-induced liposomes for cancer therapeutics. *Prog Lipid Res*. 2020;79:101052. doi:10.1016/j.plipres.2020.101052
21. Li W, Yang J, Luo L, et al. Targeting photodynamic and photothermal therapy to the endoplasmic reticulum enhances immunogenic cancer cell death. *Nat Commun*. 2019;10(1):3349. doi:10.1038/s41467-019-11269-8
22. Yang Y, Wang L, Cao H, et al. Photodynamic Therapy with Liposomes Encapsulating Photosensitizers with Aggregation-Induced Emission. *Nano Lett*. 2019;19(3):1821–1826. doi:10.1021/acsnanolett.8b04875
23. Sharma A, Liaw K, Sharma R, Zhang Z, Kannan S, Kannan RM. Targeting Mitochondrial Dysfunction and Oxidative Stress in Activated Microglia using Dendrimer-Based Therapeutics. *Theranostics*. 2018;8(20):5529–5547. doi:10.7150/thno.29039
24. Chung CH, Lu KY, Lee WC, et al. Fucoidan-based, tumor-activated nanoplateform for overcoming hypoxia and enhancing photodynamic therapy and antitumor immunity. *Biomaterials*. 2020;257:120227. doi:10.1016/j.biomaterials.2020.120227
25. Liang S, Sun C, Yang P, et al. Core-shell structured upconversion nanocrystal-dendrimer composite as a carrier for mitochondria targeting and catalase enhanced anti-cancer photodynamic therapy. *Biomaterials*. 2020;240:119850. doi:10.1016/j.biomaterials.2020.119850
26. Qindeel M, Khan D, Ahmed N, Khan S, Ur R. Surfactant-Free, Self-Assembled Nanomicelles-Based Transdermal Hydrogel for Safe and Targeted Delivery of Methotrexate against Rheumatoid Arthritis. *ACS Nano*. 2020;14(4):4662–4681. doi:10.1021/acsnano.0c00364
27. Cheng L, Kamkaew A, Sun H, et al. Dual-Modality Positron Emission Tomography/Optical Image-Guided Photodynamic Cancer Therapy with Chlorin e6-Containing Nanomicelles. *ACS Nano*. 2016;10(8):7721–7730. doi:10.1021/acsnano.6b03074
28. Li Y, Wu Q, Kang M, Song N, Wang D, Tang BZ. Boosting the photodynamic therapy efficiency by using stimuli-responsive and AIE-featured nanoparticles. *Biomaterials*. 2020;232:119749. doi:10.1016/j.biomaterials.2019.119749

29. Belali S, Savoie H, O'Brien JM, et al. Synthesis and Characterization of Temperature-Sensitive and Chemically Cross-Linked Poly (N-isopropylacrylamide)/Photosensitizer Hydrogels for Applications in Photodynamic Therapy. *Biomacromolecules*. 2018;19(5):1592–1601. doi:10.1021/acs.biomac.8b00293
30. Belali S, Karimi AR, Hadizadeh M. Cell-specific and pH-sensitive nanostructure hydrogel based on chitosan as a photosensitizer carrier for selective photodynamic therapy. *Int J Biol Macromol*. 2018;110:437–448. doi:10.1016/j.ijbiomac.2017.12.169
31. Yan J, Zhang Z, Zhan X, et al. In situ injection of dual-delivery PEG based MMP-2 sensitive hydrogels for enhanced tumor penetration and chemo-immune combination therapy. *Nanoscale*. 2021;13(21):9577–9589. doi:10.1039/d1nr01155c
32. Crommelin DJA, van Hoogevest P, Storm G. The role of liposomes in clinical nanomedicine development. *J Control Release*. 2020;318:256–263. doi:10.1016/j.jconrel.2019.12.023
33. D'Emanuele A, Attwood D. Dendrimer-drug interactions. *Adv Drug Deliv Rev*. 2005;57(15):2147–2162. doi:10.1016/j.addr.2005.09.012
34. Wu MX, Yang YW. Metal-Organic Framework (MOF)-Based Drug/Cargo Delivery and Cancer Therapy. *Adv Mater*. 2017;29:23. doi:10.1002/adma.201606134
35. Cai W, Wang J, Chu C, Chen W, Wu C, Liu G. Metal-Organic Framework-Based Stimuli-Responsive Systems for Drug Delivery. *Advanced Science*. 2019;6(1):98. doi:10.1002/advs.201801526
36. Zhang L, Gao Y, Sun S, Li Z, Wu A, Zeng L. pH-Responsive metal-organic framework encapsulated gold nanoclusters with modulated release to enhance photodynamic therapy/chemotherapy in breast cancer. *J Mater Chem B*. 2020;8(8):1739–1747. doi:10.1039/c9tb02621e
37. Zhang Y, Fu H, Chen S, Liu B, Sun W, Gao H. Construction of an iridium(III)-complex-loaded MOF nanoplatform mediated with a dual-responsive polycationic polymer for photodynamic therapy and cell imaging. *Chem Commun (Camb)*. 2020;56(5):762–765. doi:10.1039/c9cc09357e
38. Shen S, Wu Y, Liu Y, Wu D. High drug-loading nanomedicines: progress, current status, and prospects. *Int J Nanomedicine*. 2017;12:4085–4109. doi:10.2147/ijn.S132780
39. Cai W, Chu -C-C, Liu G, Wang Y-XJ. Metal-Organic Framework-Based Nanomedicine Platforms for Drug Delivery and Molecular Imaging. *Small*. 2015;11(37):4806–4822. doi:10.1002/smll.201500802
40. Horcajada P, Chalati T, Serre C, et al. Porous metal-organic-framework nanoscale carriers as a potential platform for drug delivery and imaging. *Nat Mater*. 2009;9(2):172–178. doi:10.1038/nmat2608
41. Chen G, Leng X, Luo J, et al. In Vitro Toxicity Study of a Porous Iron(III) Metal-Organic Framework. *Molecules*. 2019;24(7):58. doi:10.3390/molecules24071211
42. Paris JL, Baeza A, Vallet-Regí M. Overcoming the stability, toxicity, and biodegradation challenges of tumor stimuli-responsive inorganic nanoparticles for delivery of cancer therapeutics. *Expert Opin Drug Deliv*. 2019;16(10):1095–1112. doi:10.1080/17425247.2019.1662786
43. Yola ML, Atar N. Amperometric galectin-3 immunosensor-based gold nanoparticle-functionalized graphitic carbon nitride nanosheets and core-shell Ti-MOF@COFs composites. *Nanoscale*. 2020;12(38):19824–19832. doi:10.1039/d0nr05614f
44. Karimi-Maleh H, Yola ML, Atar N, et al. A novel detection method for organophosphorus insecticide fenamiphos: molecularly imprinted electrochemical sensor based on core-shell Co<sub>3</sub>O<sub>4</sub>@MOF-74 nanocomposite. *J Colloid Interface Sci*. 2021;592:174–185. doi:10.1016/j.jcis.2021.02.066
45. Yola ML. Sensitive sandwich-type voltammetric immunosensor for breast cancer biomarker HER2 detection based on gold nanoparticles decorated Cu-MOF and Cu<sub>2</sub>(ZnSnS<sub>4</sub>) NPs/Pt/g-C<sub>3</sub>N<sub>4</sub> composite. *Mikrochim Acta*. 2021;188(3):78. doi:10.1007/s00604-021-04735-y
46. Yola ML, Atar N. Novel voltammetric tumor necrosis factor- $\alpha$  (TNF- $\alpha$ ) immunosensor based on gold nanoparticles involved in thiol-functionalized multi-walled carbon nanotubes and bimetallic Ni/Cu-MOFs. *Anal Bioanal Chem*. 2021;413(9):2481–2492. doi:10.1007/s00216-021-03203-z
47. Lu K, He C, Lin W. Nanoscale metal-organic framework for highly effective photodynamic therapy of resistant head and neck cancer. *J Am Chem Soc*. 2014;136(48):16712–16715. doi:10.1021/ja508679h
48. Chen R, Zhang J, Wang Y, Chen X, Zapien JA, Lee CS. Graphitic carbon nitride nanosheet@metal-organic framework core-shell nanoparticles for photo-chemo combination therapy. *Nanoscale*. 2015;7(41):17299–17305. doi:10.1039/c5nr04436g
49. Li SY, Cheng H, Xie BR, et al. Cancer Cell Membrane Camouflaged Cascade Bioreactor for Cancer Targeted Starvation and Photodynamic Therapy. *ACS Nano*. 2017;11(7):7006–7018. doi:10.1021/acsnano.7b02533
50. Li SY, Cheng H, Qiu WX, et al. Cancer cell membrane-coated biomimetic platform for tumor targeted photodynamic therapy and hypoxia-amplified bioreductive therapy. *Biomaterials*. 2017;142:149–161. doi:10.1016/j.biomaterials.2017.07.026
51. Liu W, Pan Y, Zhong Y, et al. A multifunctional aminated UiO-67 metal-organic framework for enhancing antitumor cytotoxicity through bimodal drug delivery. *Chem Eng J*. 2021;412:127899. doi:10.1016/j.cej.2020.127899
52. Lu K, He C, Lin W, Chlorin-Based Nanoscale A. Metal-Organic Framework for Photodynamic Therapy of Colon Cancers. *J Am Chem Soc*. 2015;137(24):7600–7603. doi:10.1021/jacs.5b04069
53. Lan G, Ni K, Veroneau SS, et al. Titanium-Based Nanoscale Metal-Organic Framework for Type I Photodynamic Therapy. *J Am Chem Soc*. 2019;141(10):4204–4208. doi:10.1021/jacs.8b13804
54. Luo T, Ni K, Culbert A, et al. Nanoscale Metal-Organic Frameworks Stabilize Bacteriochlorins for Type I and Type II Photodynamic Therapy. *J Am Chem Soc*. 2020;142(16):7334–7339. doi:10.1021/jacs.0c02129
55. Meng HM, Hu XX, Kong GZ, et al. Aptamer-functionalized nanoscale metal-organic frameworks for targeted photodynamic therapy. *Theranostics*. 2018;8(16):4332–4344. doi:10.7150/thno.26768
56. Sun Q, Bi H, Wang Z, et al. O<sub>2</sub>-Generating Metal-Organic Framework-Based Hydrophobic Photosensitizer Delivery System for Enhanced Photodynamic Therapy. *ACS Appl Mater Interfaces*. 2019;11(40):36347–36358. doi:10.1021/acsami.9b11607
57. Wang D, Wu H, Lim WQ, et al. A Mesoporous Nanoenzyme Derived from Metal-Organic Frameworks with Endogenous Oxygen Generation to Alleviate Tumor Hypoxia for Significantly Enhanced Photodynamic Therapy. *Adv Mater*. 2019;31(27):e1901893. doi:10.1002/adma.201901893
58. Zheng Q, Liu X, Zheng Y, et al. The recent progress on metal-organic frameworks for phototherapy. *Chem Soc Rev*. 2021;50(8):5086–5125. doi:10.1039/d1cs00056j
59. Huang X, Sun X, Wang W, et al. Nanoscale metal-organic frameworks for tumor phototherapy. *J Mater Chem B*. 2021;9(18):3756–3777. doi:10.1039/d1tb00349f



60. Guan Q, Li YA, Li WY, Dong YB. Photodynamic Therapy Based on Nanoscale Metal-Organic Frameworks: from Material Design to Cancer Nanotherapeutics. *Chem Asian J.* 2018;13(21):3122–3149. doi:10.1002/asia.201801221
61. Suresh K, Matzger AJ. Enhanced Drug Delivery by Dissolution of Amorphous Drug Encapsulated in a Water Unstable Metal-Organic Framework (MOF). *Angewandte Chemie.* 2019;58(47):16790–16794. doi:10.1002/anie.201907652
62. Xue S, Zhou X, Sang W, et al. Cartilage-targeting peptide-modified dual-drug delivery nanoplatfrom with NIR laser response for osteoarthritis therapy. *Bioactive Materials.* 2021;6(8):2372–2389. doi:10.1016/j.bioactmat.2021.01.017
63. Liang J, Mazur F, Tang C, Ning X, Chandrawati R, Liang K. Peptide-induced super-assembly of biocatalytic metal-organic frameworks for programmed enzyme cascades. *Chem Sci.* 2019;10(34):7852–7858. doi:10.1039/c9sc02021g
64. Schnitzer T, Paenurk E, Trapp N, Gershoni-Poranne R, Wennemers H. Peptide-Metal Frameworks with Metal Strings Guided by Dispersion Interactions. *J Am Chem Soc.* 2021;143(2):644–648. doi:10.1021/jacs.0c11793
65. Liu X, Zhao Y, Li F. Nucleic acid-functionalized metal-organic framework for ultrasensitive immobilization-free photoelectrochemical biosensing. *Biosens Bioelectron.* 2021;173:112832. doi:10.1016/j.bios.2020.112832
66. Zhuang J, Gong H, Zhou J, et al. Targeted gene silencing in vivo by platelet membrane-coated metal-organic framework nanoparticles. *Science Advances.* 2020;6(13):eaaz6108. doi:10.1126/sciadv.aaz6108
67. Ni W, Zhang L, Zhang H, Zhang C, Jiang K, Cao X. Hierarchical MOF-on-MOF Architecture for pH/GSH-Controlled Drug Delivery and Fe-Based Chemodynamic Therapy. *Inorg Chem.* 2022;61(7):3281–3287. doi:10.1021/acs.inorgchem.1c03855
68. Eddaoudi M, Kim J, Rosi N, et al. Systematic design of pore size and functionality in isorecticular MOFs and their application in methane storage. *Science.* 2002;295(5554):469–472. doi:10.1126/science.1067208
69. Raptopoulou CP. Metal-Organic Frameworks: synthetic Methods and Potential Applications. *Materials.* 2021;14:2. doi:10.3390/ma14020310
70. Qin JH, Zhang H, Sun P, et al. Ionic liquid induced highly dense assembly of porphyrin in MOF nanosheets for photodynamic therapy. *Dalton Trans.* 2020;49(48):17772–17778. doi:10.1039/d0dt03031g
71. Zhang X, Wasson MC, Shayan M, et al. A historical perspective on porphyrin-based metal-organic frameworks and their applications. *Coord Chem Rev.* 2021;1:429. doi:10.1016/j.ccr.2020.213615
72. Chen J, Zhu Y, Kaskel S. Porphyrin-Based Metal-Organic Frameworks for Biomedical Applications. *Angewandte Chemie.* 2021;60(10):5010–5035. doi:10.1002/anie.201909880
73. Liu MD, Yu Y, Guo DK, et al. Integration of a porous coordination network and black phosphorus nanosheets for improved photodynamic therapy of tumor. *Nanoscale.* 2020;12(16):8890–8897. doi:10.1039/d0nr00956c
74. Ni D, Ferreira CA, Barnhart TE, et al. Magnetic Targeting of Nanotheranostics Enhances Cerenkov Radiation-Induced Photodynamic Therapy. *J Am Chem Soc.* 2018;140(44):14971–14979. doi:10.1021/jacs.8b09374
75. Zhang D, Ye Z, Wei L, Luo H, Xiao L. Cell Membrane-Coated Porphyrin Metal-Organic Frameworks for Cancer Cell Targeting and O (2)-Evolving Photodynamic Therapy. *ACS Appl Mater Interfaces.* 2019;11(43):39594–39602. doi:10.1021/acsami.9b14084
76. Liu TF, Feng D, Chen YP, et al. Topology-guided design and syntheses of highly stable mesoporous porphyrinic zirconium metal-organic frameworks with high surface area. *J Am Chem Soc.* 2015;137(1):413–419. doi:10.1021/ja5111317
77. Park J, Jiang Q, Feng D, Mao L, Zhou HC. Size-Controlled Synthesis of Porphyrinic Metal-Organic Framework and Functionalization for Targeted Photodynamic Therapy. *J Am Chem Soc.* 2016;138(10):3518–3525. doi:10.1021/jacs.6b00007
78. Liu Y, Zhao Y, Chen X. Bioengineering of Metal-organic Frameworks for Nanomedicine. *Theranostics.* 2019;9(11):3122–3133. doi:10.7150/thno.31918
79. Jia J, Zhang Y, Zheng M, et al. Functionalized Eu(III)-Based Nanoscale Metal-Organic Framework To Achieve Near-IR-Triggered and -Targeted Two-Photon Absorption Photodynamic Therapy. *Inorg Chem.* 2018;57(1):300–310. doi:10.1021/acs.inorgchem.7b02475
80. Liu C, Xing J, Akakuru OU, et al. Nanozymes-Engineered Metal-Organic Frameworks for Catalytic Cascades-Enhanced Synergistic Cancer Therapy. *Nano Lett.* 2019;19(8):5674–5682. doi:10.1021/acs.nanolett.9b02253
81. Pan Y, Luo Z, Wang X, et al. A versatile and multifunctional metal-organic framework nanocomposite toward chemo-photodynamic therapy. *Dalton Trans.* 2020;49(16):5291–5301. doi:10.1039/c9dt04804a
82. Cai W, Gao H, Chu C, et al. Engineering Phototheranostic Nanoscale Metal-Organic Frameworks for Multimodal Imaging-Guided Cancer Therapy. *ACS Appl Mater Interfaces.* 2017;9(3):2040–2051. doi:10.1021/acsami.6b11579
83. Gao S, Zheng P, Li Z, et al. Biomimetic O<sub>2</sub>-Evolving metal-organic framework nanoplatfrom for highly efficient photodynamic therapy against hypoxic tumor. *Biomaterials.* 2018;178:83–94. doi:10.1016/j.biomaterials.2018.06.007
84. Min H, Wang J, Qi Y, et al. Biomimetic Metal-Organic Framework Nanoparticles for Cooperative Combination of Antiangiogenesis and Photodynamic Therapy for Enhanced Efficacy. *Adv Mater.* 2019;31(15):e1808200. doi:10.1002/adma.201808200
85. Illes B, Hirschele P, Barnert S, Cauda V, Wuttke S, Engelke H. Exosome-Coated Metal-Organic Framework Nanoparticles: an Efficient Drug Delivery Platform. *Chem Materials.* 2017;29(19):8042–8046. doi:10.1021/acs.chemmater.7b02358
86. Zhang L, Cheng Q, Li C, Zeng X, Zhang XZ. Near infrared light-triggered metal ion and photodynamic therapy based on AgNPs/porphyrinic MOFs for tumors and pathogens elimination. *Biomaterials.* 2020;248:120029. doi:10.1016/j.biomaterials.2020.120029
87. Zhou Z, Wang Y, Peng F, et al. Intercalation-Activated Layered MoO<sub>3</sub> Nanobelts as Biodegradable Nanozymes for Tumor-Specific Photo-Enhanced Catalytic Therapy. *Angewandte Chemie.* 2022:e202115939. doi:10.1002/anie.202115939
88. Zhang Y, Wang F, Liu C, et al. Nanozyme Decorated Metal-Organic Frameworks for Enhanced Photodynamic Therapy. *ACS Nano.* 2018;12(1):651–661. doi:10.1021/acsnano.7b07746
89. Richter AM, Kelly B, Chow J, et al. Preliminary studies on a more effective phototoxic agent than hematoporphyrin. *J Natl Cancer Inst.* 1987;79(6):1327–1332.
90. Zeng J-Y, Zou M-Z, Zhang M, et al.  $\pi$ -Extended Benzoporphyrin-Based Metal-Organic Framework for Inhibition of Tumor Metastasis. *ACS Nano.* 2018;12(5):4630–4640. doi:10.1021/acsnano.8b01186
91. Zhang X, Huang X, Xie A, et al. Boosting type I process of Ru(II) compounds by changing tetrazole ligand for enhanced photodynamic therapy against lung cancer. *J Inorg Biochem.* 2020;212:111236. doi:10.1016/j.jinorgbio.2020.111236
92. Ke Z, Xie A, Chen J, et al. Naturally available hypericin undergoes electron transfer for type I photodynamic and photothermal synergistic therapy. *Biomater Sci.* 2020;8(9):2481–2487. doi:10.1039/d0bm00021c

93. Li M, Xiong T, Du J, et al. Superoxide Radical Photogenerator with Amplification Effect: surmounting the Achilles' Heels of Photodynamic Oncotherapy. *J Am Chem Soc.* **2019**;141(6):2695–2702. doi:10.1021/jacs.8b13141
94. Gorman A, Killoran J, O'Shea C, Kenna T, Gallagher WM, O'Shea DF. In vitro demonstration of the heavy-atom effect for photodynamic therapy. *J Am Chem Soc.* **2004**;126(34):10619–10631. doi:10.1021/ja047649e
95. Zhou LL, Guan Q, Li YA, Zhou Y, Xin YB, Dong YB. One-Pot Synthetic Approach toward Porphyrinatozinc and Heavy-Atom Involved Zr-NMOF and Its Application in Photodynamic Therapy. *Inorg Chem.* **2018**;57(6):3169–3176. doi:10.1021/acs.inorgchem.7b03204
96. Zhang K, Yu Z, Meng X, et al. A Bacteriochlorin-Based Metal-Organic Framework Nanosheet Superoxide Radical Generator for Photoacoustic Imaging-Guided Highly Efficient Photodynamic Therapy. *Adv Sci.* **2019**;6(14):1900530. doi:10.1002/adv.201900530
97. Kamkaew A, Lim SH, Lee HB, Kiew LV, Chung LY, Burgess K. BODIPY dyes in photodynamic therapy. *Chem Soc Rev.* **2013**;42(1):77–88. doi:10.1039/c2cs35216h
98. Wang W, Wang L, Li Z, Xie Z. BODIPY-containing nanoscale metal-organic frameworks for photodynamic therapy. *Chem Commun (Camb).* **2016**;52(31):5402–5405. doi:10.1039/c6cc01048b
99. Liu CX, Zhang WH, Wang N, et al. Highly Efficient Photocatalytic Degradation of Dyes by a Copper-Triazolate Metal-Organic Framework. *Chemistry.* **2018**;24(63):16804–16813. doi:10.1002/chem.201803306
100. Cai X, Xie Z, Ding B, et al. Monodispersed Copper(I)-Based Nano Metal-Organic Framework as a Biodegradable Drug Carrier with Enhanced Photodynamic Therapy Efficacy. *Adv Sci.* **2019**;6(15):1900848. doi:10.1002/adv.201900848
101. Zhao Y, Wang J, Cai X, Ding P, Lv H, Pei R. Metal-Organic Frameworks with Enhanced Photodynamic Therapy: synthesis, Erythrocyte Membrane Camouflage, and Aptamer-Targeted Aggregation. *ACS Appl Mater Interfaces.* **2020**;12(21):23697–23706. doi:10.1021/acsami.0c04363
102. Cai X, Zhao Y, Wang L, et al. Synthesis of Au@MOF core-shell hybrids for enhanced photodynamic/photothermal therapy. *J Mater Chem B.* **2021**;9(33):6646–6657. doi:10.1039/d1tb00800e
103. Luo S, Zhao Y, Pan K, et al. Microneedle-mediated delivery of MIL-100(Fe) as a tumor microenvironment-responsive biodegradable nanopatform for O(2)-evolving chemophototherapy. *Biomater Sci.* **2021**;9(20):6772–6786. doi:10.1039/d1bm00888a
104. Sun Y, Jiang X, Liu Y, et al. Recent advances in Cu(II)/Cu(I)-MOFs based nano-platforms for developing new nano-medicines. *J Inorg Biochem.* **2021**;225:111599. doi:10.1016/j.jinorgbio.2021.111599
105. Zhang W, Lu J, Gao X, et al. Enhanced Photodynamic Therapy by Reduced Levels of Intracellular Glutathione Obtained By Employing a Nano-MOF with Cu(II) as the Active Center. *Angewandte Chemie.* **2018**;57(18):4891–4896. doi:10.1002/anie.201710800
106. Wang Y, Wu W, Liu J, et al. Cancer-Cell-Activated Photodynamic Therapy Assisted by Cu(II)-Based Metal-Organic Framework. *ACS Nano.* **2019**;13(6):6879–6890. doi:10.1021/acs.nano.9b01665
107. Ni K, Lan G, Song Y, Hao Z, Lin W. Biomimetic nanoscale metal-organic framework harnesses hypoxia for effective cancer radiotherapy and immunotherapy. *Chem Sci.* **2020**;11(29):7641–7653. doi:10.1039/d0sc01949f
108. Lu J, Yang L, Zhang W, et al. Photodynamic therapy for hypoxic solid tumors via Mn-MOF as a photosensitizer. *Chem Commun (Camb).* **2019**;55(72):10792–10795. doi:10.1039/c9cc05107d
109. Meng X, Deng J, Liu F, et al. Triggered All-Active Metal Organic Framework: ferroptosis Machinery Contributes to the Apoptotic Photodynamic Antitumor Therapy. *Nano Lett.* **2019**;19(11):7866–7876. doi:10.1021/acs.nanolett.9b02904
110. Fu X, Yang Z, Deng T, et al. A natural polysaccharide mediated MOF-based Ce6 delivery system with improved biological properties for photodynamic therapy. *J Mater Chem B.* **2020**;8(7):1481–1488. doi:10.1039/c9tb02482d
111. Wang Y, Xu S, Shi L, Teh C, Qi G, Liu B. Cancer-Cell-Activated in situ Synthesis of Mitochondria-Targeting AIE Photosensitizer for Precise Photodynamic Therapy. *Angewandte Chemie.* **2021**;60(27):14945–14953. doi:10.1002/anie.202017350
112. Kan JL, Jiang Y, Xue A, et al. Surface Decorated Porphyrinic Nanoscale Metal-Organic Framework for Photodynamic Therapy. *Inorg Chem.* **2018**;57(9):5420–5428. doi:10.1021/acs.inorgchem.8b00384
113. Chen R, Chen WC, Yan L, et al. Harnessing combinational phototherapy via post-synthetic PpIX conjugation on nanoscale metal-organic frameworks. *J Mater Chem B.* **2019**;7(31):4763–4770. doi:10.1039/c9tb01154d
114. Guan Q, Zhou LL, Li YA, Dong YB. Diiodo-Bodipy-Encapsulated Nanoscale Metal-Organic Framework for pH-Driven Selective and Mitochondria Targeted Photodynamic Therapy. *Inorg Chem.* **2018**;57(16):10137–10145. doi:10.1021/acs.inorgchem.8b01316
115. Fan W, Huang P, Chen X. Overcoming the Achilles' heel of photodynamic therapy. *Chem Soc Rev.* **2016**;45(23):6488–6519. doi:10.1039/c6cs00616g
116. Casey SC, Amedei A, Aquilano K, et al. Cancer prevention and therapy through the modulation of the tumor microenvironment. *Semin Cancer Biol.* **2015**;35(Suppl):S199–S223. doi:10.1016/j.semcancer.2015.02.007
117. Wilson WR, Hay MP. Targeting hypoxia in cancer therapy. *Nat Rev Cancer.* **2011**;11(6):393–410. doi:10.1038/nrc3064
118. He L, Ni Q, Mu J, et al. Solvent-Assisted Self-Assembly of a Metal-Organic Framework Based Biocatalyst for Cascade Reaction Driven Photodynamic Therapy. *J Am Chem Soc.* **2020**;142(14):6822–6832. doi:10.1021/jacs.0c02497
119. Liu XL, Dong X, Yang SC, et al. Biomimetic Liposomal Nanoplatinum for Targeted Cancer Chemophototherapy. *Adv Sci.* **2021**;8(8):2003679. doi:10.1002/adv.202003679
120. Wang D, Wu H, Yang G, et al. Metal-Organic Framework Derived Multicomponent Nanoagent as a Reactive Oxygen Species Amplifier for Enhanced Photodynamic Therapy. *ACS Nano.* **2020**;14(10):13500–13511. doi:10.1021/acs.nano.0c05499
121. Liang R, Liu L, He H, et al. Oxygen-boosted immunogenic photodynamic therapy with gold nanocages@manganese dioxide to inhibit tumor growth and metastases. *Biomaterials.* **2018**;177:149–160. doi:10.1016/j.biomaterials.2018.05.051
122. Liu P, Zhou Y, Shi X, et al. A cyclic nano-reactor achieving enhanced photodynamic tumor therapy by reversing multiple resistances. *J Nanobiotechnology.* **2021**;19(1):149. doi:10.1186/s12951-021-00893-6
123. Ding J, Lu G, Nie W, et al. Self-Activatable Photo-Extracellular Vesicle for Synergistic Trimodal Anticancer Therapy. *Adv Mater.* **2021**;33(7):e2005562. doi:10.1002/adma.202005562
124. Liu W, Wang YM, Li YH, et al. Fluorescent Imaging-Guided Chemotherapy-and-Photodynamic Dual Therapy with Nanoscale Porphyrin Metal-Organic Framework. *Small.* **2017**;13:17. doi:10.1002/smll.201603459
125. Luo Z, Tian H, Liu L, et al. Tumor-targeted hybrid protein oxygen carrier to simultaneously enhance hypoxia-dampened chemotherapy and photodynamic therapy at a single dose. *Theranostics.* **2018**;8(13):3584–3596. doi:10.7150/thno.25409



126. Huang X, Chen T, Mu N, et al. Supramolecular micelles as multifunctional theranostic agents for synergistic photodynamic therapy and hypoxia-activated chemotherapy. *Acta biomaterialia*. 2021;131:483–492. doi:10.1016/j.actbio.2021.07.014
127. Yang G, Tian J, Chen C, et al. An oxygen self-sufficient NIR-responsive nanosystem for enhanced PDT and chemotherapy against hypoxic tumors. *Chem Sci*. 2019;10(22):5766–5772. doi:10.1039/c9sc00985j
128. Xu X, Chong Y, Liu X, et al. Multifunctional nanotheranostic gold nanocages for photoacoustic imaging guided radio/photodynamic/photothermal synergistic therapy. *Acta biomaterialia*. 2019;84:328–338. doi:10.1016/j.actbio.2018.11.043
129. Ni K, Lan G, Veroneau SS, Duan X, Song Y, Lin W. Nanoscale metal-organic frameworks for mitochondria-targeted radiotherapy-radiodynamic therapy. *Nat Commun*. 2018;9(1):4321. doi:10.1038/s41467-018-06655-7
130. Sun W, Shi T, Luo L, et al. Monodisperse and Uniform Mesoporous Silicate Nanosensitizers Achieve Low-Dose X-Ray-Induced Deep-Penetrating Photodynamic Therapy. *Adv Mater*. 2019;31(16):e1808024. doi:10.1002/adma.201808024
131. Wang Q, Liu N, Hou Z, Shi J, Su X, Sun X. Radioiodinated Persistent Luminescence Nanoplatfor for Radiation-Induced Photodynamic Therapy and Radiotherapy. *Adv Healthc Mater*. 2021;10(5):e2000802. doi:10.1002/adhm.202000802
132. Zhu Y, Shi H, Li T, et al. A Dual Functional Nanoreactor for Synergistic Starvation and Photodynamic Therapy. *ACS Appl Mater Interfaces*. 2020;12(16):18309–18318. doi:10.1021/acsami.0c01039
133. Yu Z, Zhou P, Pan W, Li N, Tang B. A biomimetic nanoreactor for synergistic chemiexcited photodynamic therapy and starvation therapy against tumor metastasis. *Nat Commun*. 2018;9(1):5044. doi:10.1038/s41467-018-07197-8
134. Luo Z, Fan X, Chen Y, et al. Mitochondria targeted composite enzyme nanogels for synergistic starvation and photodynamic therapy. *Nanoscale*. 2021;13(42):17737–17745. doi:10.1039/d1nr06214j
135. Li S, Lin K, Hu P, et al. A multifunctional nanoamplifier with self-enhanced acidity and hypoxia relief for combined photothermal/photodynamic/starvation therapy. *Int J Pharm*. 2022;611:121307. doi:10.1016/j.ijpharm.2021.121307
136. Wu X, Yang H, Chen X, et al. Nano-herb medicine and PDT induced synergistic immunotherapy for colon cancer treatment. *Biomaterials*. 2021;269:120654. doi:10.1016/j.biomaterials.2021.120654
137. Huang J, Xiao Z, An Y, et al. Nanodrug with dual-sensitivity to tumor microenvironment for immuno-sonodynamic anti-cancer therapy. *Biomaterials*. 2021;269:120636. doi:10.1016/j.biomaterials.2020.120636
138. Yang S, Zhang Z, Wang Q. Emerging therapies for small cell lung cancer. *J Hematol Oncol*. 2019;12(1):47. doi:10.1186/s13045-019-0736-3
139. Chen L, Zhou L, Wang C, et al. Tumor-Targeted Drug and CpG Delivery System for Phototherapy and Docetaxel-Enhanced Immunotherapy with Polarization toward M1-Type Macrophages on Triple Negative Breast Cancers. *Adv Mater*. 2019;31(52):e1904997. doi:10.1002/adma.201904997
140. Tian J, Xiao C, Huang B, Wang C, Zhang W. Janus macromolecular brushes for synergistic cascade-amplified photodynamic therapy and enhanced chemotherapy. *Acta biomaterialia*. 2020;101:495–506. doi:10.1016/j.actbio.2019.11.018
141. He C, Duan X, Guo N, et al. Core-shell nanoscale coordination polymers combine chemotherapy and photodynamic therapy to potentiate checkpoint blockade cancer immunotherapy. *Nat Commun*. 2016;7:12499. doi:10.1038/ncomms12499
142. Hu C, Zhuang W, Yu T, et al. Multi-stimuli responsive polymeric prodrug micelles for combined chemotherapy and photodynamic therapy. *J Mater Chem B*. 2020;8(24):5267–5279. doi:10.1039/d0tb00539h
143. Liu M, Wang L, Zheng X, Liu S, Xie Z. Hypoxia-Triggered Nanoscale Metal-Organic Frameworks for Enhanced Anticancer Activity. *ACS Appl Mater Interfaces*. 2018;10(29):24638–24647. doi:10.1021/acsami.8b07570
144. De Ruyscher D, Niedermann G, Burnet NG, Siva S, Lee AWM, Hegi-Johnson F. Radiotherapy toxicity. *Nature Reviews Disease Primers*. 2019;5(1):13. doi:10.1038/s41572-019-0064-5
145. Liu J, Yang Y, Zhu W, et al. Nanoscale metal-organic frameworks for combined photodynamic & radiation therapy in cancer treatment. *Biomaterials*. 2016;97:1–9. doi:10.1016/j.biomaterials.2016.04.034
146. Yu S, Chen Z, Zeng X, Chen X, Gu Z. Advances in nanomedicine for cancer starvation therapy. *Theranostics*. 2019;9(26):8026–8047. doi:10.7150/thno.38261
147. He T, Xu H, Zhang Y, et al. Glucose Oxidase-Instructed Traceable Self-Oxygenation/Hyperthermia Dually Enhanced Cancer Starvation Therapy. *Theranostics*. 2020;10(4):1544–1554. doi:10.7150/thno.40439
148. Wei C, Liu Y, Zhu X, et al. Iridium/ruthenium nanozyme reactors with cascade catalytic ability for synergistic oxidation therapy and starvation therapy in the treatment of breast cancer. *Biomaterials*. 2020;238:119848. doi:10.1016/j.biomaterials.2020.119848
149. De Miguel M, Calvo E. Clinical Challenges of Immune Checkpoint Inhibitors. *Cancer Cell*. 2020;38(3):326–333. doi:10.1016/j.ccell.2020.07.004
150. D'Angelo SP, Mahoney MR, Van Tine BA, et al. Nivolumab with or without ipilimumab treatment for metastatic sarcoma (Alliance A091401): two open-label, non-comparative, randomised, Phase 2 trials. *Lancet Oncol*. 2018;19(3):416–426. doi:10.1016/s1470-2045(18)30006-8
151. Lan G, Ni K, Xu Z, Veroneau SS, Song Y, Lin W. Nanoscale Metal-Organic Framework Overcomes Hypoxia for Photodynamic Therapy Primed Cancer Immunotherapy. *J Am Chem Soc*. 2018;140(17):5670–5673. doi:10.1021/jacs.8b01072
152. Shao Y, Liu B, Di Z, et al. Engineering of Upconverted Metal-Organic Frameworks for Near-Infrared Light-Triggered Combinational Photodynamic/Chemo-/Immunotherapy against Hypoxic Tumors. *J Am Chem Soc*. 2020;142(8):3939–3946. doi:10.1021/jacs.9b12788